SKELETA OF AFFINE CURVES AND SURFACES

by

SURYA THAPA MAGAR

M.A., Tribhuvan University, Nepal 2006

M.S., Kansas State University, USA 2010

AN ABSTRACT OF A DISSERTATION

submitted in partial fulfillment of the
requirements for the degree

DOCTOR OF PHILOSOPHY

Department of Mathematics
College of Arts and Sciences

KANSAS STATE UNIVERSITY
Manhattan, Kansas

2015

Abstract

A smooth affine hypersurface of complex dimension n is homotopy equivalent to a real n-dimensional cell complex. We describe a recipe of constructing such cell complex for the hypersurfaces of dimension 1 and 2, i.e. for curves and surfaces. We call such cell complex a **skeleton** of the hypersurface.

In tropical geometry, to each hypersurface, there is an associated hypersurface, called tropical hypersurface given by degenerating a family of complex amoebas. The tropical hypersurface has a structure of a polyhedral complex and it is a base of a torus fibration of the hypersurface constructed by Mikhalkin. We introduce on the edges of a tropical hypersurface an orientation given by the gradient flow of some piecewise linear function. With the help of this orientation, we choose some sections and fibers of the fibration. These sections and fibers constitute a cell complex and we prove that this complex is the skeleton by using decomposition of the coemoeba of a classical pair-of-pants. We state and prove our main results for the case of curves and surfaces in Chapters 4 and 5.

SKELETA OF COMPLEX AFFINE CURVES AND SURFACES

by

SURYA THAPA MAGAR

M.A., Tribhuvan University, Nepal, 2006

M.S., Kansas State University, USA, 2010

A DISSERTATION

submitted in partial fulfillment of the
requirements for the degree

DOCTOR OF PHILOSOPHY

Department of Mathematics
College of Arts and Sciences

KANSAS STATE UNIVERSITY
Manhattan, Kansas

2015

Approved by:

Major Professor
Dr. Ilia Zharkov

Abstract

A smooth affine hypersurface of complex dimension n is homotopy equivalent to a real n-dimensional cell complex. We describe a recipe of constructing such cell complex for the hypersurfaces of dimension 1 and 2, i.e. for curves and surfaces. We call such cell complex a **skeleton** of the hypersurface.

In tropical geometry, to each hypersurface, there is an associated hypersurface, called tropical hypersurface given by degenerating a family of complex amoebas. The tropical hypersurface has a structure of a polyhedral complex and it is a base of a torus fibration of the hypersurface constructed by Mikhalkin. We introduce on the edges of a tropical hypersurface an orientation given by the gradient flow of some piecewise linear function. With the help of this orientation, we choose some sections and fibers of the fibration. These sections and fibers constitute a cell complex and we prove that this complex is the skeleton by using decomposition of the coemoeba of a classical pair-of-pants. We state and prove our main results for the case of curves and surfaces in Chapters 4 and 5.

Table of Contents

List of Figures

Acknowledgements

I would like to express my sincere thanks to all members in the supervisory committee for my doctoral dissertation. I would like to remember them here again: Dr. Ilia Zharkov (major professor), Dr. Ricardo Castano-Bernard, Dr. Dave Auckly, Dr. Larry Weaver and Dr. Kevin Lease (outside chair person). I am indebted to you all for your time and cooperation in scheduling and making the final exam happen.

A bunch of thanks goes out to my major professor Dr. Ilia Zharkov who consistently and patiently advised, guided and mentored me for the last two years. Your availability to video chat via Skype even if you were on sabatical since last year is something I am highly appreciative of. I would also like to thank Dr. Ricardo Castano-Bernard for his continuous guidance, push and encouragement to work hard towards the completion of the dissertation. I really enjoyed all the "reading courses" I took with you. Special thanks go to Dr. Dave Auckly who was always available to help me when I asked him for, to Dr. Larry Weaver from Physics department who accepted my request in a single email to serve in the committee. Finally, same goes to Dr. Kevin Lease from Mechanical and Nuclear Engineering department for agreeing to hold final exam at the time I requested for, and most importantly for serving as outside chair in the committee.

I would like to remember my parents, Mr. Lal Thapa Magar and Mrs. Chandra Kumari Thapa for creating an inducive environment for my study since my childhood. You were, are and will be a constant source of inspiration for what I have achieved and what I will acoomplish in future. Finally, I would like to offer my big thank and love to my wife Yeera for your support to release more free time for my study and for the completion of the dissertation. Last but not the least, thanks to my cutie pie, lovely boy Nirvaan Thapa for being a happy and smiling kid all the time.

Dedication

To:

My father: **Lal Bahadur Thapa**
My mother: **Chandra Kumari Thapa**
My son: **Nirvaan Thapa.**
My wife: **Yeera Budhathoki.**

Chapter 1

Introduction

1.1 Organization and main result

In chapter 1, we give a short introduction of the 'skeleta' (a cell complex) of an smooth affine variety (in particular, an affine hypersurface) with a brief remark of the historical works done with the skeleton dating back to Lefschetz hyperplane theorem. We also give the brief account of recent works done by Ruddat, Sibilla, Treumann and Zaslow. We then digress to give a brief account of the application of skeleta in mirror symmetry and other related areas.

Chapter 2 is focused on serving background materials from tropical geometry. Starting with the definition of 'Max-Plus' semifield, We describe the process of tropicalizing a polynomial giving rise to a tropical hypersurface. We go into more details to explore the polyhedral structure of the 'tropical hypersurface'. We also state the fundamental theorem of tropical geometry.

The proof of the theorem can be found anywhere in the literature, so we skip it here. Some special properties that apply to only tropical curves are presented with some examples.

In Chapter 3, we describe the torus fibration of affine hypersurface constructed by Grigory Mikhalkin. We state definitions, lemmas and theorems from his paper [Mik04b]. For example, we define a polyhedral complex and see that the polyhedral complex with certain properties can be realized as the tropical hypersurface defined by a Laurent polynomial in 'non-Archimedean field' $\mathbb{K}^*$. Tropical hypersurfaces can be described in multiple ways: as the non-Archimedean amoeba, as the limit of a family of complex amoebas and as the spine of complex amoeba. We briefly explain the first two approaches as they are more related to this work. For the third approach done by Passare and Rullgard, we refer the reader to [PT05]. We give the definition of a topological space $V_M \subset (\mathbb{C}^*)^{n+1}$, called 'complex tropical hypersurface', which is isotopic to the original affine hypersurface V, and disscuss its properties.

Our new approach of constructing a skeleton (see Definition 4.1) using tropical geometry is the main content of chapter 4. We describe the process of obtaining skeleta for complex curves. The tropical curve is the balanced trivalent graph, see Definition 2.3. We orient using the gradient flow of a piece wise linear function the edges of the curve. Mikhalkin's torus fibration with base the tropical curve and the orientation on the curve give us a framework to build a topological cell complex. We then state and prove our result (for curve) that the complex is a skeleton of the curve 4.3.

We will give the similar construction as in Chapter 4 for surfaces in 5.

1.2 Historical Perspective

Thom gave a proof of Lefschetz Hyperplane theorem using Morse theory of critical points which is attributed to Thom in the work of Andreotti and Frankel, see [AF59]. The stronger version of the theorem is equivalent to saying that an affine smooth variety V of complex dimension n deformation retracts to a cell complex of real dimension at most n. We call the deformation retract with this property a *Skeleton* of V. Let us recall Thom's beautiful Morse-theoretic proof of Lefschetz's theorem. Fix an embedding $V \subseteq \mathbb{C}^N$, and let $\rho : V \to \mathbb{R}$ be the function that measures the distance to a fixed point $p \in \mathbb{C}^N$. For a generic choice of p, this is a plurisubharmonic Morse function, so its critical points cannot have index greater than n. The skeleton of V is the union of stable submanifolds of the gradient flow of ρ. However, finding an explicit description of these stable submanifolds requires one to solve some differential equations.

1.3 RSTZ Version of Skeleta

Ruddat, Sibilla, Truemann and Zaslow [RSTZ] in [RSTZ14] described the recipe for constructing skeleta for affine hypersurface in an affine toric variety. The construction is based on the combinatorics of the Newton polytope of the defining polynomial.

Let $f : (\mathbb{C}^*)^{n+1} \to \mathbb{C}$ be a Laurent polynomial defined by

$$f(z) = \sum_{m \in \Delta \subset \mathbb{Z}^{n+1}} a_m z^m$$

where $m = (m_1, \ldots, m_{n+1}) \in \mathbb{Z}^{n+1}$ and $z^m = z_1^{m_1} \ldots z_{n+1}^{m_{n+1}}$. Denote the zero locus defined by $f(z)$ as $V(f) = \{z \in (\mathbb{C}^*)^{n+1} : f(z) = 0\}$. The Newton polytope, Δ of f is the convex hull of the set of $m \in \mathbb{Z}^{n+1}$ where the coefficient a_m of f is non zero. If the coefficients a_m are chosen generically, the diffeomorphism type of $V(f)$ depends only on the Newton polytope of f. In fact, it suffices that the coefficients corresponding to the vertices of the Newton polytope are chosen generically. More precisely,

Proposition 1.1. *([GKZ94], Chapter 10, Cor 1.7). Let $A \in \mathbb{Z}^{n+1}$ be a finite set whose affine span is $\mathbb{Z}^{n+1}$, and let f_A be a Laurent polynomial of the form*

$$f(z) = \sum_{m \in A} a_m z^m$$

There is a Zariski open dense subset $U_A \subseteq \mathbb{C}^{|A|}$ such that, when the coeffi-

cients $a_m, m \in A$ are chosen from U_A, the variety $V(f_A)$ is smooth and its diffeomorphism type depends only on the convex hull of A.

Definition 1.1. An intersection of a finitely many linear affine half spaces in a finite-dimensional vector space is called *Polyhedron*. A compact polyhedron is called *polytope*. A polytope can also be defined as the convex hull of finite number of points called vertices.

We let M denote a free abelian group isomorphic to $\mathbb{Z}^{n+1}$ and set $M_{\mathbb{R}} = M \otimes_{\mathbb{Z}} \mathbb{R} \cong \mathbb{R}^{n+1}$. A polytope $\Delta \subseteq M_{\mathbb{R}}$ is called a *lattice polytope* if its vertices are in M. Let $\partial\Delta$ denote the boundary of Δ. A lattice triangulation T_Δ of a polytope Δ is a triangulation by lattice simplices. Such triangulation is called regular or coherent if there is a piecewise affine convex function $h : \Delta \to \mathbb{R}$ such that the (maximal) closed domain where h is linear coincides with the maximal simplex in T_Δ.

Definition 1.2. Let $\Delta \subseteq \mathbb{R}^{n+1}$ be a lattice polytope with $0 \in \Delta$. Let T_Δ be a star triangulation based at 0 (that means every maximal simplex contains origin) of Δ, and define T to be the set of simplices of T_Δ not meeting 0. Write $\partial\Delta'$ for the support of T. Define

$$S_{\Delta,T} \subseteq \partial\Delta' \times \mathrm{Hom}(\mathbb{Z}^{n+1}, S^1)$$

to be the set of pairs (x, ϕ) satisfying the following condition:

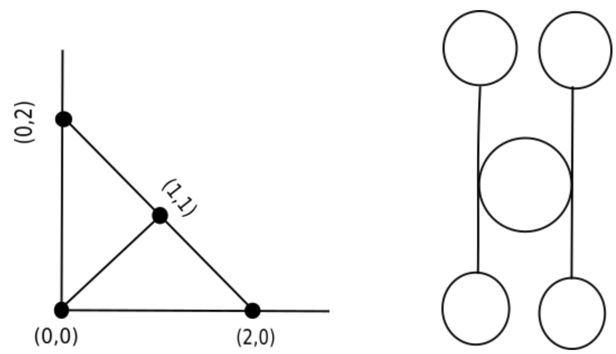

Figure 1.1: Star triangulation of Δ and a skeleton S of $f = -1 + xy + x^2 + y^2$ in $\mathbb{C}^* \times \mathbb{C}^*$

.

$\phi(v) = 1$ whenever v is a vertex of the smallest simplex $\tau \in T$ containing x. Denote $S := S_{\Delta,T}$.

Theorem 1.2 (RSTZ [RSTZ14]). *Let Δ and T be as in Definition 1.2. Let V be a generic smooth hypersurface whose Newton polytope is Δ. If T is regular, then S embeds into V as a deformation retract and is called a skeleton of V.*

Example 1.1. Consider a Laurent polynomial $f = -1 + xy + x^2 + y^2$ and $Z = V(f)$ in $\mathbb{C}^* \times \mathbb{C}^*$. We define $\phi \in \mathrm{Hom}(\mathbb{Z}^2, \mathbb{R}/\mathbb{Z}$ such that $\phi = (\alpha, \beta)$, where $\phi(u, v) = \alpha u + \beta v \mod \mathbb{Z}$. At vertex $(2, 0)$, $\phi(u, v) = \{(\alpha, \beta) : 2\alpha = 0\} \cong \mathbb{Z}/2 \times \mathbb{Z}/2$. So, α is 0 or $1/2$ and β is free, which is homeomorphic to two disjoints circles. Similarly, at vertex $(0, 2)$, there are two disjoint circles: α is free and β is 0 or $1/2$. Along the line segment $(2, 0) - (1, 1)$, it is two points: $(\alpha, \beta) = (0, 0)$ or $(1/2, 1/2)$. Over $(1, 1)$, it is a single circle $\beta = -\alpha$.

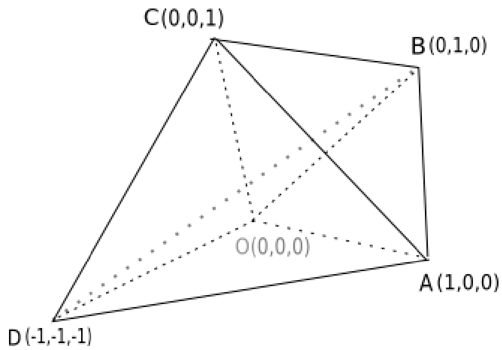

(a) Newton polytope of the quartic $ax + by + cz + \frac{d}{xyz} + e = 0$ in $\mathbb{C}^* \times \mathbb{C}^* \times \mathbb{C}^*$. It has a unique star triangulation T_Δ with respect to origin.

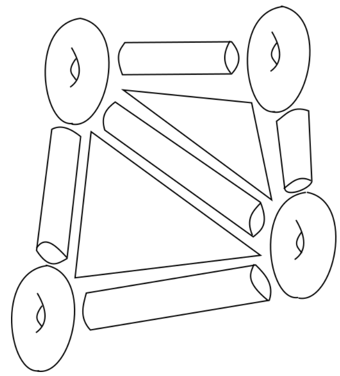

(b) A part of the skeleton of 1.2a. Each cylinder meeting one of the tori $S^1 \times S^1$ is attached along a different circle. There is a sixth cylinder and two additional triangles BCD and ABD in Figure 1.2a

Figure 1.2: Skeleton of a Quartic surface.

So, $S_{\Delta,T}$ is homotopic to a bouquet of five circles, see Figure 1.1.

For proof of the theorem, they used the coherent triangulation of the Newton polytope, which means there is a piecewise linear function from Δ to $\mathbb{R}$. Using this function, they constructed a degeneration of the ambient space $(\mathbb{C}^*)^{n+1}$ and with it, the degeneration of the hypersurface V. Each component of the degeneration is the space $(\mathbb{C}^*)^{n+1}$. The degenerated hypersurface deformation retracts onto a simple locus which can be triangulated explicitly. In each component, the top-dimensional simplices of this triangulation are the non-negetive loci of the components. Then they used Log geometry to account for the topological difference between the degenerated hypersurface and the general one, see [RSTZ14].

RSTZ version of a skeleton depends on the 'star triangulation' of the Newton polytope of the defining polynomial. Our work would to some extent, address the issues of finding skeleta that doesn't depend on the particular choice of the triangulation of the Newton polytope. So, our novel approach of finding the skeleta using tropical geometry is independent of any triangulation and hence makes no contact with the techniques RSTZ applied in [RSTZ14].

1.4 Related Work

Recently skeleton of a variety has seen its appearance in mirror symmetry which is a very active area of research in mathematics and theoretical physics (string theory). Mirror symmetry relates the complex geometry of one Calabi-Yau manifold to the symplectic geometry of other Calabi-Yau (CY) manifold and vice versa. This pair of manifolds is called mirror pair. This idea was formalized by Kontsevich [Kon94] in 1994 on the language of homological algebra. He conjectured that mirror symmetry could be interpreted as an equivalence of two categories : bounded derived category of coherent sheaf on one CY manifold and the derived Fukaya category on the mirror manifold. Results in support of the conjecture have been found in some cases such as elliptic curve, K3 surface and abelian varieties. Kontsevich later proposed an extension of the conjecture to cover some fano varieties where the mirror of a fano variety is Landau-Ginzburg model i.e. an affine variety equipped with a holomorphic function called superpotential. The symplectic side of Landau-Ginzburg model is the Fukaya-Seidel category. More recently, Katzarkov and others [KKOY09] proposed another extension of the conjecture to cover some varieties of general type.

One fundamental object of interest in the mirror symmetry is Fukaya category. This is a category associated to a sympletic manifold, whose objects are compact lagrangian submanifolds satisfying certain transversality property and with some additional structures. The morphism between two objects is Floer complex generated by the intersection points between two Lagrangian submanifolds. The Floer complex is equipped with a differential which counts weighted holomorphic discs bounded by the Lagrangians. Several modifications have been made with the original Fukaya categories to accommodate those modifications in homological mirror symmetry conjecture. Of particular interest is to include non-compact Lagrangian submanifolds as objects in the Fukaya category. This modification is made by some pertubations of Lagrangians at infinity giving rise to wrapped Fukaya categories and constructible sheaves.

For a Stein manifold X, Paul Seidel in his book “Fukaya Categories and

Picard-Lefschetz Theory" described the Fukaya category in terms of Lefschetz fibrations. One can analyze his construction and associate a certain algebra A of finite type so that the Fukaya category constructed by Seidel is a full subcategory of Fin(A), a homotopy category of dg-modules. Kontsevich in [Kon09] conjectured that X can be contracted to singular Lagrangian skeleton $L \subset X$ so that A depends only on L and Fin(A) is a global category associated with constructible sheaf of smooth dg categories on the skeleton L.

When $\triangle$ and $\triangle^{\wedge}$ are a pair of reflexive polytopes, Batyrev and Borisov [Bat94], [Bor93] explain how to construct from them a pair of smooth projective Calabi-Yau hyperserfaces . Let $\mathbf{P}_{\triangle}$ and $\mathbf{P}^{\wedge}_{\triangle}$ be the associated projective toric varieties. The skeleta and constructible sheaves appear at the large volume/large complex structure limits of these families of hypersurfaces. Let $\mathbf{Z}$ and $\mathbf{Z}^{\wedge}$ be the 'large volume limit' and 'large complex structure limit', of mirror pair. In [FLTZ11] a relation was found between coherent sheaves on a toric variety and a subcategory of constructible sheaves on a real torus. The subcategory is defined by conical Lagrangian $\wedge$ in the cotangent bundle of the torus. This conical Lagrangian is homotopy equivalent to the Legendrian $\wedge^{\infty}$ at contact infinity of the cotangent bundle. $\wedge^{\infty}$ is the skeleton of $\mathbf{Z}$ and supports a Kashiwara-Schapira sheaf of dg categories [TZ11]. This sheaf is equivalent to the 'constructible plumbing model' of [STZ11] and should be equivalent to perfect complexes on $\mathbf{Z}^\wedge$ as shown in [STZ11]. It is conjectured in [TZ11] that under homological mirror symmetry the 'constructible plumbing model' on $\wedge^\infty$ is equivalent to the sheaf of Fukaya categories, conjectured to exist by Kontsevich [Kon09], supported on the skeleton of $\mathbf{Z}$. When $\triangle$ and $\triangle^\wedge$ are both reflexive and simplicial, it is conjectured in [TZ11] that $\wedge^\infty$ is the skeleton of $\mathbf{Z}^\wedge$.

Chapter 2

Tropical Geometry

In this chapter, we discuss the definition and some fundamendal aspects of tropical geometry. The basic notion in tropical geometry is *tropical semi-ring*, which is also called max-plus semi-ring. We can do algebraic geometry over this semi-ring and algebraic varieties correspond to "tropical varieties" in this geometry. Tropical varieties are combinatorial in nature and actually are 'polyhedral complexes'. They are assumed to retain some properties of algebraic varieties and have been successfully used to understand more about their counterpart in (enumerative) algebraic geometry.

For basic notions and related topics in tropical geometry, we refer to Mikhalkin's surveys [Mik06]. To learn introductory materials and recent advances in tropical geometry, we refer to the book 'Introduction to Tropical Geometry' by Maclagan and Sturmfels, [MS15].

2.1 Tropical Semi-field

As a set, *tropical semi-field* $\mathbb{T} = (\mathbb{R} \cup \{-\infty\}, \oplus, \odot)$ is the real number $\mathbb{R}$, together with an extra element $-\infty$ that represents negetive infinity. However, the arithmatic operations of tropical addition $\oplus$ and tropical multiplication $\odot$ of real numbers are defined as follows:

$$x \oplus y := \max(x, y) \qquad \text{and} \qquad x \odot y := x + y.$$

Many of the familiar axioms remain valid in tropical operations. For instance, both addition and multiplication are commutative: $x \oplus y = y \oplus x \quad \text{and} \quad x \odot y = y \odot x$. The distributive law holds for tropical multiplication over tropical addition: $x \odot (x \oplus y) = x \odot y \oplus x \odot y$. The neutral elements for addition and multiplication also exist. $x \oplus -\infty = x \quad \text{and} \quad x \odot 0 = x$. However, there is no 'subtraction' in tropical arithmetic. There is no solution to $10 \oplus x = 6$ for all x. Tropical division is defined to be the classical subtraction. The set $\mathbb{T} = (\mathbb{R} \cup \{-\infty\}, \oplus, \odot)$ satisfies all axioms of field except the existance of additive inverse. So $\mathbb{T}$ is called tropical semi-field. A very important feature of the tropical semi-field is that $\oplus$ is idempotent, which means $x \oplus x = x$.

2.2 Maslov Dequantization

The tropical semi-field arises naturally as the limit of some classical semi-fields. This can be seen by the process known as Maslov dequantization of positive real numbers.

Let $\mathbb{R}_{\geq 0}$ denote the semi-field of positive real numbers under usual addition and multiplication. Let t be a real number greater than 1, then the logarithm of base t provides a bijection between the sets: $\mathbb{R}_{\geq 0}$ and $\mathbb{T}$. This bijection induces a semi-field structure on $\mathbb{T}$ with the operations denoted by $\oplus_t$ and $\odot_t$ and defined by:

$$x \oplus_t y = \log_t(t^x + t^y) \qquad \text{and} \qquad x \odot_t y = \log_t(t^x t^y) = x + y.$$

The second equation above already shows classical addition arising from the multiplication on $(\mathbb{R}_{\geq 0}, +, \times)$. All semi-fields $(\mathbb{T}, \oplus_t, \odot_t)$ are isomorphic to $(\mathbb{R}_{\geq 0}, +, \times)$ by construction. The inequalities $\max(x, y) \leq x+y \leq 2\max(x, y)$ on $\mathbb{R}_{\geq 0}$ together with the fact that the logarithm of base $t > 1$ is an increasing function gives us the following bounds for $\oplus_t$:

$$\max(x, y) \leq x \oplus_t y \leq \max(x, y) + \log_t 2.$$

$\log_t 2$ tends to 0 as $t \to \infty$, and the operation $\oplus_t$ therefore tends to the tropical addtition $\oplus$. Hence the tropical semi-field (ring) comes naturally from degenerating classical semi-fields $(\mathbb{R}_{\geq 0}, +, \times)$.

2.3 Tropical Polynomial

Let $x_1, \dots, x_n$ be n variables that represent elements in the tropical semi-field $\mathbb{T}$. A tropical monomial is any product of these variables, where repetition is allowed, $a \odot x_1^{i_1} \odot \cdots \odot x_n^{i_n}$. Here the coefficient a is real number and the exponents $m_1, \dots, m_n$ are integers. Tropical monomials are the linear functions with integer coefficients because $x_1^{i_1} = x_1 \odot x_1 \odot \cdots \odot x_1 (i_1 \text{ factors}) = i_1 x_1$. A tropical polynomial is a finite linear combination of tropical monomials:

$$P(x_1, \dots, x_n) = a_1 \odot x_1^{i_{11}} \odot \cdots \odot x_n^{i_{1n}} \oplus a_2 \odot x_1^{i_{21}} \odot \cdots \odot x_n^{i_{2n}} \oplus \dots$$
$$\oplus\, a_m x_1^{i_{m1}} \odot \cdots \odot x_n^{i_{mn}}, a_i \in \mathbb{Z}$$

Every tropical polynomial represents a function $P : \mathbb{R}^n \to \mathbb{R}$. Evaluating this function in classical arithmetic, we get the maximum of a finite collection of linear functions.

$$P(x_1, \dots, x_n) = \max\{a_1 + i_{11}x_1 + \cdots + i_{1n}x_n, a_2 + i_{21}x_1 + \cdots + i_{2n}x_n, \dots,$$
$$a_m + i_{m1}x_1 + \cdots + i_{mn}x_n\}.$$

This function $P : \mathbb{R}^n \to \mathbb{R}$ has important properties:

- P is continuous.
- P is piecewise-linear.
- P is concave,

Thus the tropical polynomials in n variables $x_1, x_2, \dots x_n$ are precisely the piecewise-linear concave functions in $\mathbb{R}^n$ with integer coefficients. Some examples of tropical polynomials in one variable: $1 \oplus x = \max(1, x)$, $1 \oplus x \oplus 3 \odot x^2 = \max(1, x, 2x+3)$ $1 \oplus x \oplus 3 \odot x^2 \oplus (-2) \odot x^3 = \max(1, x, 2x+3, 3x-2)$ We define the *tropical roots* of the tropical polonomial $P(x) = \bigoplus_{i=1}^{d}(a_i \odot x^i)$ in one variable as points x_0 of $\mathbb{T}$ for which the graph of $P(x)$ has a 'corner' (where $P(x)$ fails to be linear) at x_0. This is equivalent to $P(x_0)$ being equal to the value of at least two of its monomials evaluated at x_0. The difference in the slopes of the two pieces adjacent to the corner gives the order of the corresponding root.

2.4 Tropical Curve in $\mathbb{R}^2$

Now we describe some properties of tropical curve.

Definition 2.1. A *tropical polynomial* in two variables is

$$P(x, y) = \oplus_{(i,j) \in A} a_{i,j} \odot x^i \odot y^j = \max_{(i,j) \in A}(a_{i,j} + ix + jy),$$

where A is a finite subset of $(\mathbb{Z}_{\geq 0})^2$. A tropical polynomial is a concave piecewise linear function as stated above. The tropical curve, Γ_{trop} defined by $P(x, y)$ is defined as the corner locus (where $P(x, y)$ fails to be linear) of this function or equivalently the set of points where the function is not

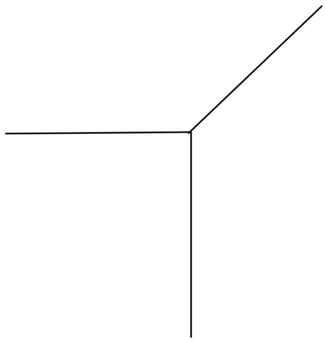

(a) $x \oplus y \oplus 0$

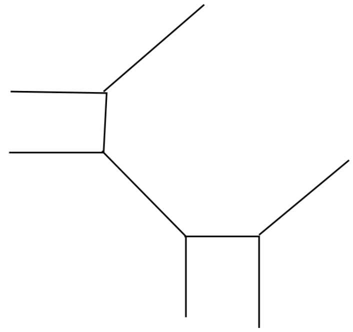

(b) $3 \oplus 2 \odot x \oplus 2 \odot y \oplus 3 \odot x \odot y \oplus y^2 \oplus x^2 \oplus 0$

Figure 2.1: A tropical line and a tropical conic

smooth. Moreover, $\Gamma_{\text{trop}} = \{(x, y) \in \mathbb{R}^2 \ : \ (x, y) \text{ is achieved twice}\}$.

Example 2.1. Consider a tropical line defined by the polynomial $P(x, y) = x \oplus y \oplus 0$. Γ_{trop} is given by:

$$x = 0 \geq y, \qquad y = 0 \geq x, \qquad x = y \geq 0.$$

We see that Γ_{trop} consists of three standard half-lines (see Figure 2.1a): $\{(x, 0) \in \mathbb{R}^2 : x \leq 0\}$, $\{(0, y) \in \mathbb{R}^2 : y \leq 0\}$. and $\{(x, y) \in \mathbb{R}^2 : x = y \geq 0\}$.

The set Γ_{trop} is a trivalent graph in $\mathbb{R}^2$.

Definition 2.2. Let $P(x, y)$ be a tropical polynomial and Γ_{trop} its associated tropical curve. The weight of an edge of Γ_{trop} is defined as the maximum of the greatest common divisor (gcd) of the numbers $|i-k|$ and $|j-l|$ such that the value of $P(x,y)$ on this edge is maximum for $a_{i,j}x^iy^j$ and $a_{k,l}x^ky^l$ monomials.

So, the tropical curve Γ_{trop} is equipped with the weight function defined on its edges.

2.5 Newton polytope and its dual subdivision

The Newton polytope of a polynomial in two variables $P(x,y) = \sum_{(i,j)} a_{ij}x^iy^j$, denoted by $\Delta(P)$ is given by,

$$\Delta(P) = \text{conv}\{(i,j) \in (\mathbb{Z}_{\geq 0})^2 : a_{ij} \neq 0\} \subset \mathbb{R}^2.$$

A tropical polynomial determines a subdivision of $\Delta(P)$, called its *dual subdivision*. Given $(x_0, y_0) \in \mathbb{R}^2$, let

$$\Delta_{(x_0,y_0)} = \text{conv}\{(i,j) \in \mathbb{Z}^2_{\geq 0} : P(x_0,y_0) = a_{ij} \odot x_0^i \odot y_0^j\} \in \Delta(P)$$

The tropical curve Γ_{trop} defined by $P(x,y)$ induces a polyhedral decomposition of $\mathbb{R}^2$ and the polytope $\Delta(x_0,y_0)$ only depends on the cell $F : (x_0,y_0) \in F$ of the decomposition given by Γ_{trop}. Thus we define $\Delta_F = \Delta_{(x_0,y_0)}$ for $(x_0,y_0) \in F$.

Example 2.2. Consider the tropical line L defined by the polynomial: $P(x,y) =$

(a) (b)

Figure 2.2: Subdivision dual to tropical curves depicted in Figure 2.1

$x \oplus y \oplus 0 = \max\{x, y, 0\}$, see Figure 2.1a. For the 2-cell F_1, where $P(x, y)$ is maximum given by monomial 0, $\Delta_{F_1} = \text{conv}\{(0, 0)\}$. Similarly, we have $\Delta_{F_2} = \text{conv}\{(1, 0)\}$ and $\Delta_{F_3} = \text{conv}\{(0, 1)\}$ for the cells F_2 where x assumes maximum value and F_3 where y assumes maximum value respectively. Along the horizontal edge e_1, where $P(x, y)$ is maximum given by 0 and y, $\Delta_{e_1} = \text{conv}\{(0, 0), (0, 1)\}$. In the same way, $\Delta_{e_2} = \text{conv}\{(0, 0), (1, 0)\}$ and $\Delta_{e_3} = \text{conv}\{(1, 0), (0, 1)\}$. For the vertex v, where the monomials 0, x and y assume maximum value, $\Delta_v = \text{conv}\{(0, 0), (1, 0), (0, 1)\}$.

For all cells F, the polyhedra Δ_F form a subdivision of the Newton polytope $\Delta(P)$. This subdivision is dual to the tropical curve defined by $P(x, y)$ in the following sense.

Proposition 2.1. *One has*

- $\Delta(P) = \cup_F \Delta_F$, *where the union is taken over all cells F of the polyhedral subdivision of $\mathbb{R}^2$ induced by the tropical curve defined by $P(x, y)$;*
- *dim F = codim Δ_F;*
- $\Delta_F \subset \Delta_{F'}$ *if and only if $F' \subset F$;*

(a) (b) Δ_v

Figure 2.3: Balancing condition: the numbers 1 and 3 indicate the weight of an edge.

- *$\Delta_F \subset \partial\Delta(P)$ if and only of F is unbounded.*

Furthermore, one can show that the weight of an edge of a tropical curve can be seen from the dual subdivision.

Proposition 2.2. *An edge e of a tropical curve has weight w if and only if the integer length of Δ_e is $w = \mathrm{car}(\Delta_e \cap \mathbb{Z}^2) - 1$.*

Proof. See [Mik05]. $\square$

2.6 Balanced graphs and tropical curves

Let v be a vertex of a tropical curve Γ_{trop}, and let $e_1, \ldots, e_k$ be the edges adjacent to v. Let their weights be $w_1, \ldots, w_k$. Let $v_i, i = 1, \ldots, k$ be the primitive integral vector in the direction of e_i and pointing outward from v, see Figure 2.3.

Definition 2.3. (Balancing condition): With the above notations, at each vertex v of Γ_{trop}, one has

$$\sum_{i=1}^{k} w_i v_i = 0.$$

A rectilinear graph $\Gamma \in \mathbb{R}^2$ whose edges have rational slopes and are equipped with positive integer weights is called a *balanced graph* if Γ satisfies the balancing condition at each vertex. We have seen that every tropical curve is a balanced graph. The converse is also true.

Theorem 2.3 ([Mik04a])**.** *Any balanced graph in $\mathbb{R}^2$ is a tropical curve.*

2.7 Tropical curve as the limit of amoebas

Tropical curve can be treated as a certain limit of amoebas of algebraic curves in $(\mathbb{C}^*)^2$. This is true for n-dimensional hypersurfaces which will be explained in Chapter 3. Now we will explain the 2-dimensional case. Consider the map (for $t > 1$);

$$\begin{aligned} \mathrm{Log}_t : \ (\mathbb{C}^*)^2 \quad & \longrightarrow \quad \mathbb{R}^2 \\ (z, w) \quad & \longmapsto \quad (\log_t |z|, \log_t |w|). \end{aligned}$$

Definition 2.4 ([GKZ94])**.** The amoeba (in base t) of an algebraic curve $V \in (\mathbb{C}^*)^2$ is the image $\mathrm{Log}_t(V)$ of V under Log_t.

For example, the amoeba of the line $L \subset (\mathbb{C}^*)^2$ of the polynomial $z+w+1 = 0$ is shown in Figure 2.4. The amoeba has three asymptotic directions

$(-1,0),(0,-1)$and$(1,1)$. The amoeba of L in base t is a contraction by a factor of $\log(t)$ of the amoeba of L in base e (see Figure 2.4). When t approaches $+\infty$, the amoeba is contracted to the limit which is the tropical line given as the corner locus of $f(x,y) = \max\{0, x, y\}$. This process of amoebas degeneration equally applies to any curve in $(\mathbb{C}^*)^2$ and to any complex affine hypersurface in higher dimension.

Example 2.3. Here is another example of a family of amoebas defined by $1 - z - w + t^2z^2 - t^{-1}zw + t^{-2}w^2 = 0$ degenerating to the limiting object, which is a tropical conic, see Figure 2.5.

2.8 Fundamental Theorem of Tropical Geometry

Consider a field $\mathbb{K}$ with a valuation, val : $\mathbb{K}^* \to \mathbf{R}$, where $\mathbb{K}^* = \mathbb{K}\backslash\{0\}$ and val satisfies these properties:

1. $\text{val}(ab) = \text{val}(a) + \text{val}(b)$
2. $\text{val}(a+b) \leq \max(\text{val}(a), \text{val}(b))$. The function val can be extended to $\mathbb{K}$ by defining $\text{val}(0) = -\infty$

Example 2.4. 1. $\mathbb{K} = \mathbb{C}$ with the trivial valuation, $\text{val}(a) = 0$ for all $a \in \mathbb{C}^*$.

2. $\mathbb{K}$ the field of Puiseux series. The elements of $\mathbb{K}$ are given by $b \in \mathbb{K}^*, b = \sum_{j\in\mathbb{R}} a^j t^j,\ j \to \infty, a_j \in \mathbb{C}^*$. A valuation is given by taking $a \in \mathbb{C}\{\{t\}\}$

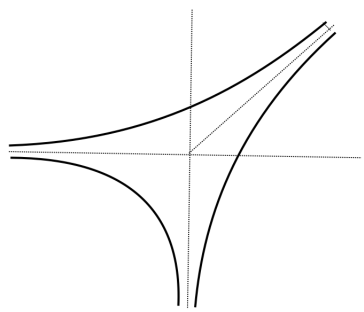

(a) $\mathrm{Log}(L)$

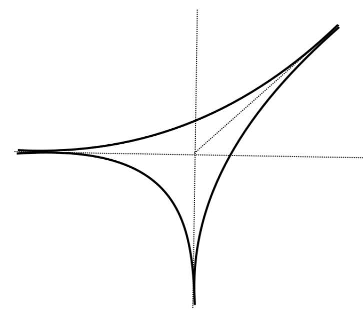

(b) $\mathrm{Log}_{t_1}(L)$

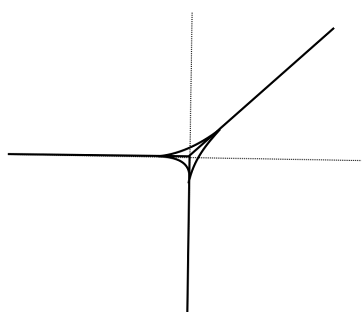

(c) $\mathrm{Log}_{t_2}(L)$

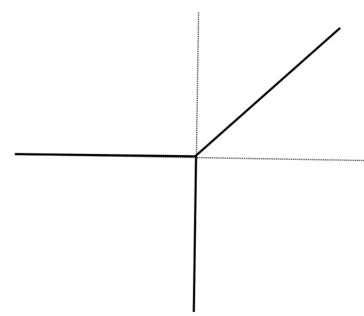

(d) $\lim_{t\to\infty}\mathrm{Log}_t(L)$

Figure 2.4: Degeneration of amoeba to a tropical curve in the case of 2-dimensional pair-of-pants ($e < t_1 < t_2$).

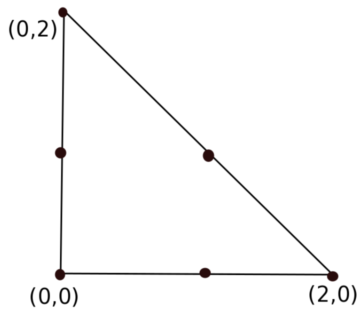

(a) Newton polytope of a conic

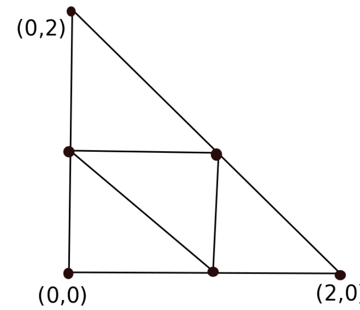

(b) Subdivision dual to tropical curve 2.5d

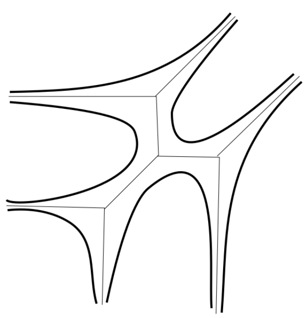

(c) Amoeba of the conic

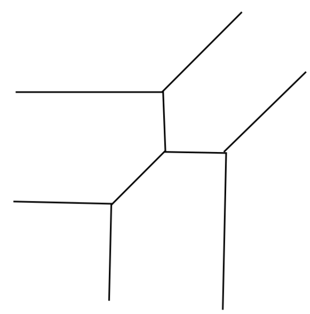

(d) Tropical conic

Figure 2.5: Amoeba and tropical conic of $1 - z - w + t^2 z^2 - t^{-1} zw + t^{-2} w^2 = 0$.

to be the lowest exponent appearing. For example $\mathrm{val}(3t^{-1/2}+8t^2+7t^{13/2}+\dots)=-1/2$.

Definition 2.5. The tropicalization of a Laurent polynomial $f=\sum c_u x^u \in \mathbb{K}[x_1^{\pm 1},\dots,x_n^{\pm 1}]$ is $\mathrm{trop}(f):\mathbb{R}^n \to \mathbb{R}$ given by:

$$\mathrm{trop}(f)(w)=\max(\mathrm{val}(c_u)+w.u),$$

where maximum is taken over all $\{u\in\mathbb{Z}^n : c_u\neq 0\}$ and $w.u$ denotes the standard scaler product of $\mathbb{R}^n$.

For $f\in\mathbb{K}[x_1^{\pm 1},\dots,x_n^{\pm 1}]$, the hypersurface $V(f)$ is the zero set of the polynomial f. That is $V(f)=\{x\in(\mathbb{K}^*)^n : f(x)=0\}$. The tropicalization $\mathrm{trop}(V(f))$ of $V(f)$ is the tropical hypersurface defined by trop(f). This tropical hypersurface is the corner locus of trop(f), or equivalently,

$$\mathrm{trop}(V(f))=\{w\in\mathbb{R}^n : \text{the max in } \mathrm{trop}(f) \text{ is achieved at least twice}\}.$$

The tropicalization of a variety $Y\subset(\mathbb{K}^*)^n$ generated by an ideal $I=<f_1,\dots,f_r>,\ f_i\in\mathbb{K}[x_1^{\pm 1},\dots,x_n^{\pm 1}],\ \forall i$ is

$$\mathrm{trop}(Y)=\bigcap_{f\in I}\mathrm{trop}(V(f)).$$

Example 2.5. Let $Y=V(t^3x^3+x^2y+xy^2+t^3y^3+x^2+t^{-1}xy+y^2+x+y+t^3)\subseteq(\mathbb{C}\{\{t\}\}^*)^2$. The $\mathrm{trop}(V(f))$ is shown in Figure 2.6 which is a "tropical

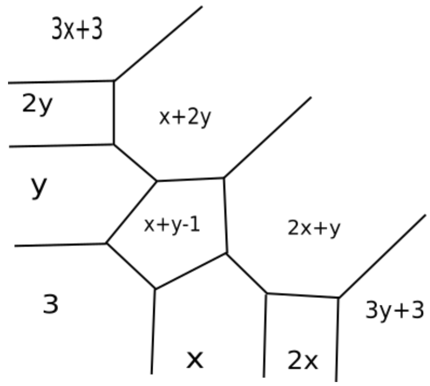

Figure 2.6: Tropical elliptic curve

elliptic curve".

Theorem 2.4. *(*Fundamental theorem of tropical geometry*). Let K be an algebraically closed field with a non trivial valuation* val : $\mathbb{K}^* \to \mathbb{R}$*, and let Y be a subvariety of $(\mathbb{K}^*)^n$ defined by an ideal I. Then the following sets coincide.*

- trop(Y)*.*
- *The closure in $\mathbb{R}^n$ of $\{w \in (\mathrm{Im}(\mathrm{val}))^n : \mathrm{in}_w(I) \neq 1\}$.*
- *The closure in $\mathbb{R}^n$ of $\{\mathrm{Val}(y) : y \in Y\}$.*

Here, $\mathrm{in}_w(I)$ is the initial form of an ideal. Val is the map from $(\mathbb{K}^*)^n$ to $\mathbb{R}^n$ with coordinate-wise valuation map.

Proof. See [MS15]. A particular case of this theorem applied to an affine hypersurface is known as Kapranov's theorem [see Chapter 3].

$\square$

Example 2.6. Let $Y = V(x+y+1) \subseteq (\mathbb{K}^*)^2$, where $\mathbb{K} = \mathbb{C}\{\{t\}\}$.

Then $Y = \{(a, -1-a) : a \in \mathbb{K}^* \backslash \{-1\}\}$. Note that

$$(\mathrm{val}(a), \mathrm{val}(-1-a)) = \begin{cases} (\mathrm{val}(a), 0) : & \mathrm{val}(a) < 0 \\ (\mathrm{val}(a), \mathrm{val}(a)) : & \mathrm{val}(a) > 0 \\ (0, \mathrm{val}(b)) : & a = -1+b, \mathrm{val}(b) < 0 \\ (0, 0) : & \text{otherwise} \end{cases}$$

And the graph is the same as in Figure 2.1a. This proves that the two sets; first and third from the fundamental theorem coincide.

Chapter 3

Torus fibration of an affine hypersurface

In this chapter, we discuss the Mikhalkin's construction of torus fibration of algebraic hypersurface from his paper [Mik04b]. The base of the torus fibration is its associated tropical hypersurface, which was defined in Chapter 2. This fibration can be seen as a pair-of-pants decomposition of the hypersurface. We first define an n-dimensional pair-of-pants P_n, the primitive complex Σ_n and give a fibration $\lambda_H : P_n \to \Sigma_n$. The fibration λ_H gives a local picture of the pair-of-pant decomposition of the hypersurface. We explain proper gluing conditions to put these local fibrations together to construct a global fibration of the hypersurface.This is formulated in the proof of Theorem 3.11.

Following [Mik04b] and [NS11], we define a complex space $V_M \subset (\mathbb{C}^*)^{n+1}$

called "complex tropical hypersurface" as the limit of a family of holomorphic hypersurfaces parametrized by the self-diffeomorphism $H_t : (\mathbb{C}^*)^{n+1} \to (\mathbb{C}^*)^{n+1}$. We also describe an alternative way of defining V_M, which is more suited for our works to build the 'skeleton'.

3.1 Polyhedral Complex

A polyhedron P in $\mathbb{R}^n$ is the intersection of finitely many half-spaces in $\mathbb{R}^n$. This is given by a set of linear inequalities as:

$$P = \{x \in \mathbb{R}^n : Ax \leq b\},$$

where A is a $d \times n$- matrix and $b \in \mathbb{R}^d$. We say that P is rational if A and b have rational entries.

If $b = 0$, then P is called a cone, in which case there exists a finite set of linearly independent points $v_1, \ldots, v_s$ such that $P = \text{conv}(v_1, \ldots, v_s) := \{\sum_{i=1}^{s} \lambda_i v_i : \lambda_i \geq 0\}$.

Polyhedral Complex: A subset $\Pi \in \mathbb{R}^{n+1}$ is called a *proper rational polyhedral complex* if it is a finite union of closed sets in $\mathbb{R}^{n+1}$ called *cells* satisfying the following properties.

- Each cell is closed (some may be semi-infinite) convex polyhedron. The dimension of the cell is the dimension of the smallest affine space which contains it. We call a cell of dimension k a k-cell.

- The slope of affine span of each cell is rational
- The boundary of a k-cell is the union of $(k-1)$-cells.
- The intersection of two $k-$cells is also a cell of the complex or empty.
- Different open cells (interiors of the cells in the corresponding affine span) do not intersect.

Essentially, a proper polyhedral complex in $\mathbb{R}^{n+1}$ is a cellular space where each cell is a convex polyhedron with a rational slope. The dimension of the complex is the maximal dimension of the affine span of its cells. If each polyhedron in the complex is a cone, then the complex is called a fan.

Definition 3.1. A polyhedral n-complex is called *weighted* if there is a natural number $w(F)$ prescribed to each of its n-cells F.

A weighted polyhedral n-complex $\Pi \in \mathbb{R}^{n+}$ is called *balanced* if for every $(n-1)$-cell $G \in \Pi$ the following condition holds: Let $F_1, \ldots, F_k$ be the n-cells adjacent to G and $c(F_1), \ldots, c(F_m)$ their weights. The balancing condition is :

$$\sum_{j=1}^{k} c(F_j) = 0$$

Example 3.1. Consider a piecewise linear function $H : \mathbb{R}^{n+1} \to \mathbb{R}$ defined by:

$$H(x_1, \ldots, x_{n+1}) = \max\{0, x_1, \ldots, x_{n+1}\}$$

We denote the 'corner locus' of this function by $\Sigma_n \subset \mathbb{R}^{n+1}$. Corner locust implies the set of points where H is not smooth. Σ_n is a balanced proper rational polyhedral complex in $\mathbb{R}^{n+1}$. Its k-cell is formed by the points where any $n+2-k$ functions of $n+2$ functions, $0, x_1, \ldots, x_{n+1}$ achieve maximum value for H.

Let $A \subset \mathbb{Z}^{n+1}$ be a finite set and let $v : A \to \mathbb{R}$ be any function. Let $\Delta \subset \mathbb{R}^{n+1}$ be the convex hull of A. The **Legendre transform** of v is defined by $L_v : \mathbb{R}^{n+1} \to \mathbb{R}$,

$$L_v(y) = \max_{x \in A}\{< x, y > -v(x)\}.$$

where $x, y \in \mathbb{R}^{n+1}$ and $< x, y >$ is the scaler product in $\mathbb{R}^{n+1}$. Since the maximum is taken over a finite set, L_v is a convex piecewise linear function. We define a polyhedral complex Π_v as the corner locus of L_v.

We below state some propositions from [Mik04b], which characterize the complex Π_v defined in Example 3.1.

Proposition 3.1. *The set Π_v is a balanced proper rational polyhedral complex dual to a certain lattice subdivision of Δ.*

The converse of the Proposition 3.1 is also true.

Proposition 3.2. *Suppose that* $\Pi \subset \mathbb{R}^{n+1}$ *is a weighted balanced proper rational polyhedral complex. Then there exists a finite set* $A \in \mathbb{Z}^{n+1}$ *and a function* $v : A \to \mathbb{R}$ *such that* $\Pi = \Pi_v$. *The convex hull* $\Delta \in \mathbb{R}^{n+1}$ *of* A *is unique upto a translation in* $\mathbb{Z}^{n+1}$.

Definition 3.2. We call Π a dual Δ-complex if it corresponds to Π_v as defined in Proposition 3.2. The polyhedral complex Π is called maximal if the elements in the corresponding subdivision of Δ are simplices of volume $\frac{1}{(n+1)!}$. The triangulation of Δ with this property is called *unimodular triangulation*.

The following two Propositions 3.3 and 3.4 from [Mik04b] characterize and relate Σ_n to the standard simplex Δ_1.

Proposition 3.3. *Any lattice polytope of volume* $\frac{1}{(n+1)!}$ *can be identified with the standard simplex* Δ_1 *by an element of* $ASL_{n+1}(\mathbb{Z})$.

Here $ASL_{n+1}(\mathbb{Z})$ stands for the group of affine linear transformation or $\mathbb{R}^{n+1}$.

Proposition 3.4. *Any dual* Δ_1*-complex is the result of a translation of* Σ_n *in* $\mathbb{R}^{n+1}$.

Proposition 3.5. *Denote by* Π *a balanced proper maximal polyhedral complex. Let* $U_j \subset \Pi$ *to be a neighborhood of a vertex* $v_j \in \Pi$. *For each* U_j, *there* *exists $M_j \in ASL_{n+1}(\mathbb{Z})$ such that $M_j(U_j) \in \Sigma_n$ is an open set containing origin in the primitive complex Σ_n.*

3.2 Fibration of a pair-of-pants

The section provides the definition of an n-dimensional pair-of-pants and the construction of a fibration of the pair-of-pants, where the base of the fibration is Σ_n.

Definition 3.3. The space $P_n = \mathbb{CP}^{n+1}\backslash\{n+2 \text{ generic hyperplanes}\}$ is called n-dimensional pair-of-pants. If we choose coordinates of $\mathbb{CP}^{n+1}$ as $(z_0, z_1, \ldots, z_{n+1})$ and take coordinate planes as generic hyperplanes, P_n can be identified with the affine hypersurface H° in $(\mathbb{C}^*)^{n+1}$ defined by $1 + z_1 + z_2 + \cdots + z_{n+1} = 0$. For simplicity, we have taken $z_0 = 1$.

Let $\mathrm{Log} : \mathbb{C}^{n+1} \to \mathbb{R}^{n+1}$ be a map defined by

$$\mathrm{Log}(z_1, \ldots, z_{n+1}) = (\log|z_1|, \ldots, \log|z_{n+1}|)$$

Lemma 3.6. $\Sigma_n \subset \mathrm{Log}(H^\circ)$

Proof. According to [PR04], Σ_n is a spine of the amoeba $\mathrm{Log}(H^\circ)$ $\square$

The complement $\mathbb{R}^{n+1}\backslash\Sigma_n$ consists of $n+2$ components corresponding to one of the functions $0, x_1, \ldots, x_{n+1}$ being maximal. In the component corresponding to x_j, we consider the foliation of the component into straight lines parallel to the gradient of x_j. In the component corresponding to 0, we consider the foliation into straight lines parallel to $(1, \ldots, 1)$. These foliations glue together to form a foliation of $\mathbb{R}^{n+1}$, call it F. Define a projection $\pi_F : \mathbb{R}^{n+1} \to \Sigma_n$ along these leaves (the straight lines).

Lemma 3.7. *The map $\lambda_H := \pi_F \circ Log : H^\circ \to \Sigma_n$ is a fibration of P_n, where λ_H restricted to an open n-cell of Σ_n is a trivial n-torus fibration, see Figure 3.1.*

Definition 3.4. Now we define a Viro's patchworking polynomial. Let $v : \Delta \cap \mathbb{Z}^{n+1} \to \mathbb{R}$ be any function and $a(z) = \sum_{j \in \Delta \cap \mathbb{Z}^{n+1}} a_j z^j$ be any polynomial. For any $t > 0$, Viro's patchworking polynomial is defined by

$$f_t^v(z) = \sum_{j \in \Delta \cap \mathbb{Z}^{n+1}} a_j t^{-v(j)} z^j,$$

where $a_j \neq 0$ for any $j \in \Delta \cap \mathbb{Z}^{n+1}$.

Consider $V_f \subset (\mathbb{C}^*)^{n+1}$ as the zero locus of a Laurent polynomial

$$f(z) = \sum_{j \in \Delta} a_j z^j, \qquad z^j = z_1^{j_1} \ldots z_{n+1}^{j_{n+1}},$$

where $\Delta \subset \mathbb{Z}^{n+1}$ is the Newton polytope. Recalling the definition of *Amoeba* A_f of a variety, $V_f \subset (\mathbb{C}^*)^{n+1}$,

an amoeba of a variety over the non-Archimedean field can be similarly defined. Let K be a non-Archimedean field with a valuation map val, see

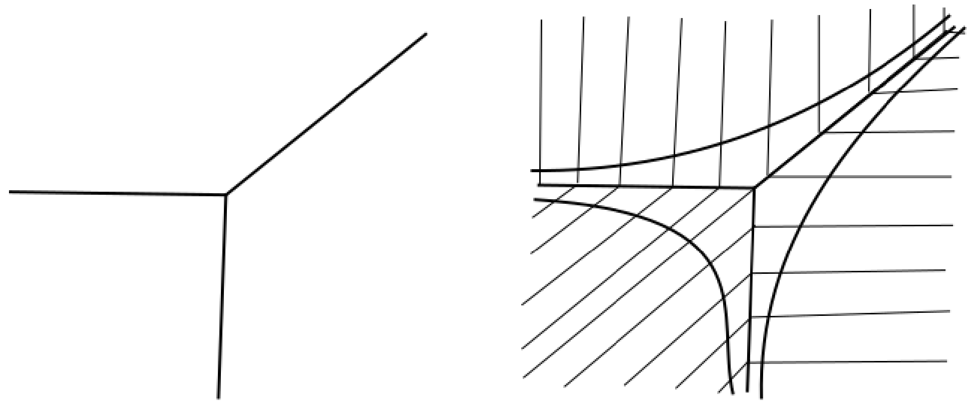

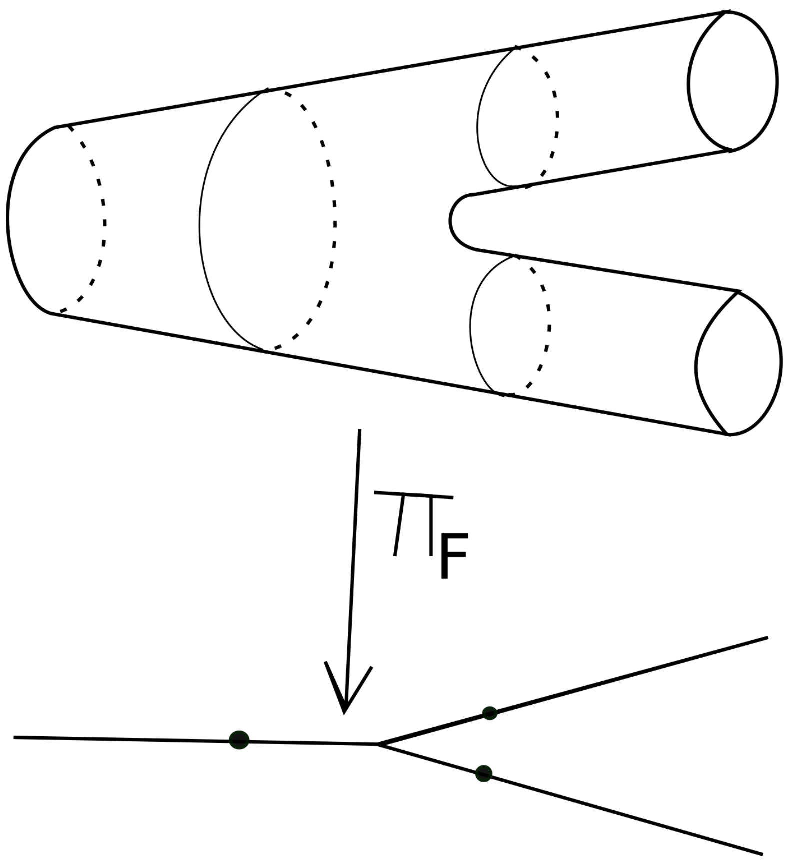

Figure 3.1: fibration P_1 over Σ_1.

Example 2.4. Note that e^{val} gives a norm on K. Define the map

$$\mathrm{Log}_K : (\mathbb{K}^*)^{n+1} \to \mathbb{R}^{n+1}$$

$$\mathrm{Log}_K(z_1, \ldots, z_{n+1}) = (\log|z_1|_K, \ldots, \log|z_{n+1}|_K),$$

where $|.|_K$ is the norm in K given by e^{val}. Let $V_K \subset (\mathbb{K}^*)^{n+1}$ be any affine hypersurface. The amoeba of V_K is the image of V_K under the map Log_K. Such amoeba is called *non-Archimedean amoeba.* Kapranov's theorem shows that the non-Archimedean amoebas are balanced polyhedral complex.

Theorem 3.8. *([Kapranov]) If $V_K \subset (\mathbb{K}^*)^{n+1}$ is a hypersurface given by $f = \sum a_j z^j$, $a_j \in \mathbb{K}^*$, then the non-Archimedean amoeba $\mathrm{Log}(V_K)$ is the balanced polyhedral complex corresponding to the function $v(j) = val(a_j)$ defined on the lattice points of the Newton polytope Δ of V_K.*

Under tropicalization, the non-Archimedean amoeba is the corner locus of the tropical polynomial defined by

$$f(x) = \max_{j\in\Delta}\{\mathrm{val}(a_j) + < x, j >\}.$$

Let $f_t = \sum_{j\in\Delta\cap\mathbb{Z}^{n+1}} a_j t^{-v(j)} z^j$, $t > 0$ be a general patchworking polynomial. Denote $V_t := \{f_t = 0\} \in (\mathbb{C}^*)^{n+1}$. The coefficients $a_j t^{-v(j)}$ of f_t can be considered as elements of $\mathbb{K}$, the non-Archimedean field of Puiseux series and hence the family f_t can be considered as a single polynomial in

$(\mathbb{K}^*)^{n+1}$. It defines a hypersurface $V_{\mathbb{K}} \in (\mathbb{K}^*)^{n+1}$. Denote $A_t := \mathrm{Log}_t(V_t)$ and $A_K := \mathrm{Log}_{\mathbb{K}}(V_{\mathbb{K}})$. Recall that *the Hausdorff distance* between two closed subsets $A, B \subset \mathbb{R}^{n+1}$ is the number

$$\max\{\sup_{a\in A} d(a,B), \sup_{b\in B} d(b,A)\},$$

where $d(a,B)$ is the Euclidean distance between a point a and a set B in $\mathbb{R}^{n+1}$.

Corollary 3.9. *The amoeba A_t converges in the Hausdorff metric to the non-Archimedean amoeba A_K when $t \to \infty$.*

Proof. See [Mik04b] □

Let $F \subset \Pi$ be an open $(n+2-k)$-cell. F is dual to a k-dimensional polytope from the subdivision of Δ. Since Π is maximal, this polytope is the standard $(k-1)$ - simplex upto an action of $ASL_{n+1}(\mathbb{Z})$. Then one can show

Lemma 3.10. *There exists k monomials $t^{-v(j_1)}z^{j_1}, \ldots, t^{-v(j_k)}z^{j_k}$ that dominate f_t in a neighborhood of F. Furthermore, the hypersurface*

$$\sum_{m=1}^{k} t^{-v(jm)} z^{j_m} = 0$$

is isomorphic to the hyperplane $z_1 + \cdots + z_{k-1} + 1 = 0$ under the multiplicative change of coordinates by an element of $ASL_{n+1}(\mathbb{Z})$.

The theorem below is Mikhalkin's pair-of-pants decomposition of $V_t \subset$

$(\mathbb{C}^*)^{n+1}$.

Theorem 3.11 (Mikhalkin). *For every maximal dual Δ-complex Π there exists a stratified T^n-fibration $\lambda : V \to \Pi$ such that for each primitive piece U_j of Π, the inverse image $(\lambda^{-1}(U_j)$ is an open pair-of-pants P_n.*

Proof. See [Mik04a] for the proof.

□

3.3 Complex Tropical Hypersurfaces

Let t be a strictly positive real number and H_t be the self-diffeomorphism of $(\mathbb{C}^*)^{n+1}$ defined by:

$$\begin{array}{rccc} H_t: & (\mathbb{C}^*)^{n+1} & \longrightarrow & (\mathbb{C}^*)^{n+1} \\ & (z_1, \dots, z_{n+1}) & \longmapsto & (t^{-|z_1|}\dfrac{z_1}{|z_1|}, \dots t^{-|z_{n+1}|}\dfrac{z_{n+1}}{|z_{n+1}|}). \end{array}$$

H_t defines a new complex structure on $(\mathbb{C}^*)^{n+1}$ denoted by $J_t = (dH_t) \circ J \circ (dH_t)^{-1}$ where J is the standard complex structure. A J_t-holomorphic hypersurface V_t is a hypersurface holomorphic with respect to the J_t complex structure on $(\mathbb{C}^*)^{n+1}$. It is equivalent to say that $V_t = H_t(V)$ for some $V \subset (\mathbb{C}^*)^{n+1}$ holomorphic hypersurface with respect to the standard complex structure J.

Definition 3.5. Let $V \subset (\mathbb{C}^*)^{n+1}$ be a hypersurface defined by a Laurent polynomial $f(z) = \sum_{j\in\Delta} a_j z^j$, Δ is the Newton polytope. A complex tropical hypersurface $V_\infty \subset (\mathbb{C}^*)^{n+1}$ is the limit (with respect to Hausdorff metric on compact sets in $(\mathbb{C}^*)^{n+1}$) of a sequence of J_t-holomorphic hypersurfaces $V_t \in (\mathbb{C}^*)^{n+1}$ when $t \to \infty$.

3.4 Phase tropical hypersurface

There is another way of describing V_∞ through a pair of maps: Namely, using the tropicalization and argument on a non-Archimedean field with a valuation. Mounir Nisse and Frank Sottile in [NS11] called V_∞'Phase Tropical Hypersurface'.

Let $\mathbb{K}^*$ be a field with non-Archimedean valuation $\mathrm{val} : \mathbb{K}^* \to \mathbb{R}$ as defined in Example 2.4. For now, let $\mathbb{K}^*$ be the field of Puiseux series, $\mathbb{K}^*$, which is algebraically closed. Let $b \in \mathbb{K}^*$ be such that $b = \sum_{j\in J} b_j t^j$ where $b_j \in \mathbb{C}^*$ and $J \subset \mathbb{R}$ is partially ordered and bounded below. Then $\mathrm{val}(b) = -\min\{j : b_j \neq 0\}$. Also define a map $\phi : \mathbb{K}^* \to S^1$ by $\phi(b) = \arg(b_{-\mathrm{val}(b_j)})$. That means ϕ takes the argument of the coefficient at the lowest power of t. This is a homomorphism from the multiplicative group $\mathbb{K}^*$ to S^1. Combined with valuation map, this defines a homomorphism $w : \mathbb{K}^* \to \mathbb{C}^* \approx \mathbb{R} \times S^1$ such that $w(b) = (\mathrm{val}(b), \phi(b))$. This induces a homomomorphism $W : (\mathbb{K}^*)^{n+1} \to (\mathbb{C}^*)^{n+1}$.

Lemma 3.12. *If $V_K \subset (\mathbb{K}^*)^{n+1}$ is a hypersurface given by a polynomial*

$f = \sum a_j z^j$, $a_j \in \mathbb{K}^*$ *then* $W(V_K) \subset (\mathbb{C}^*)^{n+1}$ *depends only on the values* $w(a_j) \in \mathbb{C}^*$.

Proof. Proof is easy. From Kapranov's theorem 3.8, $\mathrm{Log}(W(V_K)) = \mathrm{Log}_K(V_K)$. So one only needs to show that $u(a_j)$ determines the arguments of $W(V_K)$ see [Mik04b]. $\square$

Let $V_t \subset (\mathbb{C}^*)^{n+1}$ be a family of hypersurfaces defined by a general patchworking polynomial $f_t = \sum_{j\in\Delta} a_j t^{-v(j)} z^j$. If we denote $a_j t^{-v(j)} = b_j$, then $b_j \in \mathbb{K}^*$, f_t can be considered as a single polynomial in $(\mathbb{K}^*)^{n+1}$. Let $V_{\mathbb{K}} \subset (\mathbb{K}^*)^{n+1}$ be the hypersurface defined by the polynomial f_t. V_∞ can be described in terms of the lifts of non-Archimedean amoebas to $(\mathbb{C}^*)^{n+1}$.

Theorem 3.13 (Mikhalkin)**.** *The sets* $H_t(V_t)$ *converge in the Hausdorff metric to* $W(V_{\mathbb{K}})$ *when* $t \to \infty$.

Proof. See [Mik04b]. $\square$

The map W can be understood as the product of a pair of maps, Tropicalization and Argument. Thus by Theorem 3.13 V_∞ is seen as the closure of the image of V_K under that product map. This allows to give a more geometric description of V_∞. It is a certain $2n$-dimensional object in $(\mathbb{C}^*)^{n+1}$ which projects down to tropical hypersurface under Log. And hence the diagram below is commutative..

If $\mathrm{Log} : (\mathbb{C}^*)^{n+1} \to \mathbb{R}^{n+1}$ be the map defined by $\mathrm{Log}(z_1, \ldots, w_{n+1}) = (\log|z_1|, \ldots, \log|w_{n+1}|)$. Then we have

$$\mathrm{Log} \circ H_t = \mathrm{Log}_t.$$

H_t corresponds to the contraction by $\log(t)$, $(x_1, \ldots, x_{n+1}) \mapsto (\frac{x_1}{\log(t)}, \ldots, \frac{x_{n+1}}{\log(t)})$ under Log.

$$\begin{tikzcd}
(\mathbb{K}^*)^{n+1} \arrow[r, "\mathrm{W}"] \arrow[d, "\mathrm{Val}"'] & (\mathbb{C}^*)^{n+1} \arrow[d, "H_t"] \arrow[dl, "\mathrm{Log}_t"'] \\
\mathbb{R}^{n+1} & (\mathbb{C}^*)^{n+1} \arrow[l, "\mathrm{Log}"]
\end{tikzcd}$$

Let $\mathrm{Arg} : (\mathbb{C}^*)^{n+1} \to S^1 \times \cdots \times S^1$ be defined by: $\mathrm{Arg}(z_1, \ldots, z_{n+1}) = (\arg(z_1), \ldots \arg(z_{n+1}))$.

The following proposition from [Mik05] further characterizes the complex tropical hypersurface V_∞. It gives a description of local structure of V_∞.

Let $V_f \subset (\mathbb{C}^*)^{n+1}$ be an affine hypersurface defined by: $f(z) = \sum_{j \in \Delta} a^j z^j$, Δ is Newton polytope. Let V_{trop} and V_∞ be the corresponding tropical hypersurface and complex tropical hypersurface respectively. V_{trop} induces a lattice subdivision of Δ. We also have two projection maps, $\mathrm{Log} : V_\infty \to V_{\mathrm{trop}}$ and

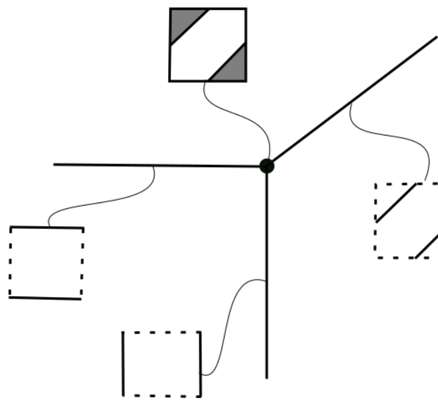

Figure 3.2: Complex tropical line $z_1 + z_2 + 1 = 0$.

$\mathrm{Arg} : V_\infty \to T^n$

Proposition 3.14. *Let* $x \in V_{trop}$ *and* $\tau \subset V_{trop}$ *be the cell of smallest dimension which contains* x*. Let* Δ' *be the polytope in the subdivision of* Δ *dual to* τ*. Then* $\mathrm{Arg}(\mathrm{Log}^{-1}(x) \cap V_\infty) = \mathrm{Arg}(V^{'})$ *for some* $V^{'} \subset (\mathbb{C}^*)^{n+1}$ *with the Newton polytope* $\Delta^{'}$*.*

Thus we can think of $V_\infty = W(V_K^\circ)$ both as the tropical hypersurface equipped with a *phase* and as the limit of J_t-holomorphic hypersurfaces when $t \to \infty$.

For example, Figure 3.2 represents a complex tropical line $z_1 + z_2 + 1 = 0$ in $\mathbb{R}^2$. Consider the dual subdivision of its Newton polytope, which is standard 2-simplex. The fiber of Log of a point on the horizontal edge is $\mathrm{Arg}(z_2 + 1 = 0) \subset \mathbb{T}^2$, on the slant edge is $\mathrm{Arg}(z_1 + z_2 = 0) \subset \mathbb{T}^2$ and over the vertex is $\mathrm{Arg}(z_1 + z_2 + 1 = 0) \subset \mathbb{T}^2$. Topologically, this line is homeomorphic to P_1.

3.5 Coamoeba of P_n

Definition 3.6. The coamoeba is the image of a subvariety of a complex torus $(\mathbb{C}^*)^{n+1}$ under the argument map Arg. The geometric and combinatorial structure of the coamoeba of a hypersurface with the Newton polytope a simplex had been studied in [Nis11]. We describe below such structure of the coamoeba of H° defined by $z_1 + z_2 + \cdots + z_{n+1} = 0$ in $(\mathbb{C}^*)^{n+1}$. The proof of our main theorem 5.3 relies on the decomposition of this coamoeba into polytopes.

A hypersurface $H \subset (\mathbb{C}^*)^{n+1}$ whose Newton polytope is a unimodular simplex is a hyperplane and is defined by the polynomial

$$1 + a_1 z_1 + \cdots + a_{n+1} z_{n+1} = 0. \tag{3.1}$$

Definition 3.7. The coamoeba $coA(H)$ of H is the image of H under the map Arg.

Changing coordinates in Equation 3.1 from $a_i z_i$ to x_i transforms Equation 3.1 to

$$1 + x_1 + \cdots + x_{n+1} = 0 \tag{3.2}$$

The coamoeba of 3.1 is the translation of the coamoeba of 3.2 by the vector $(\arg(a_1), \arg(a_2), \ldots \arg(n+1))$

Chapter 4

Construction Of Skeleta: Curve Case

Let $V_f \subset (\mathbb{C}^*)^2$ be a smooth affine curve defined by a Laurent polynomial $f(z_1, z_2) = \sum_{(i,j)\in\Delta} a_{ij} z_1^i z_2^j$, where Δ is the Newton polytope. We consider a coherent triangulation of Δ, given by upper convex hull of the graph of the map $\gamma : \Delta \cap \mathbb{Z}^2 \to \mathbb{R}$. We assume that the triangulation of Δ is unimodular. Let $f_t(z_1, z_2) = \sum_{(i,j)\in\Delta} a_{ij} t^{-\gamma(i,j)} z_1^i z_2^j$ be a general patchworking polynomial. f_t gives a family of affine curves V_t and V_t gives a family of amoebas A_t. We know A_t degenerates as $t \to \infty$ to a tropical curve V_{trop} and V_t to a complex tropical curve V_∞. We put V_M for V_∞ for simplicity.

V_{trop} is a balanced trivalent graph, where some of the edges may extend to ∞.

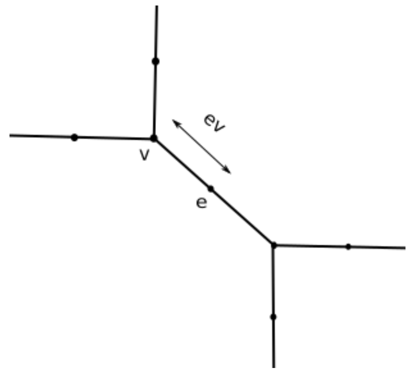

Figure 4.1: 'v' 'e' and 'ev' of the barycentric subdivision.

4.1 Barycentric subdivision and notation

Consider the barycentric subdivision, $\mathbf{bsd}(V_{\text{trop}})$ of V_{trop}. Denote by 'v' and 'e' (barycenter of edge E) the vertices and by 'ev' or 've' the edge from 'v' to 'e' in the subdivision.

4.2 Orientation on the graph V_{trop}

To construct the skeleton, we need an orientation of barycentric subdivision of V_{trop} such that

1. At each 'v', one of the 'ev' edges is oriented in (call it incoming) and the other two oriented out (call it outgoing).
2. At each 'e', at most one 'ev' is outgoing.
3. For the infinite ends, we need them to be oriented from ∞ to 'e'.
4. the graph is acyclic.

4.3 Construction of the orientation

We give two constructions of the orientation with the properties described above. We consider a generic piece-wise concave linear function $\Phi : \mathbb{R}^2 \to \mathbb{R}$. The gradient flow of Φ induces an orientation on the edges of the barycentric subdivision. This orientation can have:

At ‘e’: Two incident edges can have the following possible orientations.

1. One ‘ev’ is incoming and the other outgoing. This happens when Φ gets its maximum value at end of ‘E’.

2. Both ‘ev’ are incoming. This is possible when Φ achieves maximum value at ‘e’. In this case, we call this ‘e’ as ‘marked e’.

3. Note that both ‘ev’ cannot be incoming at ‘e’ because Φ is concave and has no minimum.

At ‘v’: Three ‘E’ edges (or ‘ev’ edges) incident at ‘v’ could be oriented as follows.

1. One ‘ev’ incoming and other two outgoing. This occurs when Φ assumes maximum value at ‘v’ for the incoming ‘E’. This is the orientation we want to have.

2. Two ‘ev’s are incoming and the other one outgoing. This occurs when Φ assumes maximum value at ‘v’ for two incoming ‘E’s. In this case,

we switch the orientation of one of the incoming 'ev' edges. This switch gives rise to 'marked e'.

3. All 'ev's are incoming or all are outgoing. Both cannot happen due to balancing condition Γ_{trop} satisfies at each 'v'.

All 'ev' incoming or all 'ev' outgoing at 'v' cannot happen due to balancing condition at each 'v' of the tropical curve. Let e_1, e_2, e_3 be the integral vectors along the direction of 'ev's. Then $\Phi(e_1) + \Phi(e_2) + \Phi(e_3) = \Phi(e_1 + e_2 + e_3) = \Phi(0) = 0$. So, $\Phi(e_1), \Phi(e_2)$ and $\Phi(e_3)$ cannot have all positives or all negetives.

Lemma 4.1. *The graph with oriented 'ev' edges described above is acyclic.*

Proof. There are no cycles of edges before we make switches of the orientation of some 'ev's because the arrows always point towards increasing of Φ. It won't have such cycles either after the switch because a potential cycle cannot pass through 'marked e'. $\square$

Another example is'distance function'. Let $E_1^\infty, E_2^\infty, \ldots, E_r^\infty$ denote the infinite edges from V_{trop}. Consider a finite set of points,

$$P = \{p_i \in E_i^\infty \ : \ p_i \text{ is an interior point of } E_i^\infty\}$$

Consider the function $\Phi : V_{\text{trop}} \to \mathbb{R}$ which is the distance of a point in V_{trop} to the set P.

We can choose the set P general enough so that the maximum value of the function do not occur at vertices of the graph.

For the generic choice of P, the gradient flow of Φ induces an orientation on V_{trop} with the properties:

- One edge is incoming and the other two outgoing at each vertex.
- At an edge, there are at most one 'ev' is outgoing.
- We re-orient infinite edges going from ∞ to p_i.

Because this orientation is given by the gradient flow of a function, it is acyclic.

Define the set: $Q := \{x \in V_{\text{trop}} :$ when two local gradient flows meet$\}$. Equivalently, Q is the set of 'marked e' vertices.

Proposition 4.2 ([Zha10]). *The cardinality of set Q is equal to $g - 1 + \{$cardinality of $P\}$.*

4.4 Coamoeba of P_1

P_1 is a line given by $az_1 + bz_2 + c = 0$ with $a, b, c \in \mathbb{C}^*$, replacing z_1 by cz_1'/a and z_2 by cz_2'/b to obtain the line $z_1' + z_2' + 1 = 0$, with coamoeba as in Figure 4.2 . This transformation rotates the coamoeba 4.2 by arg(a/c) horizontally and arg(b/c) vertically.

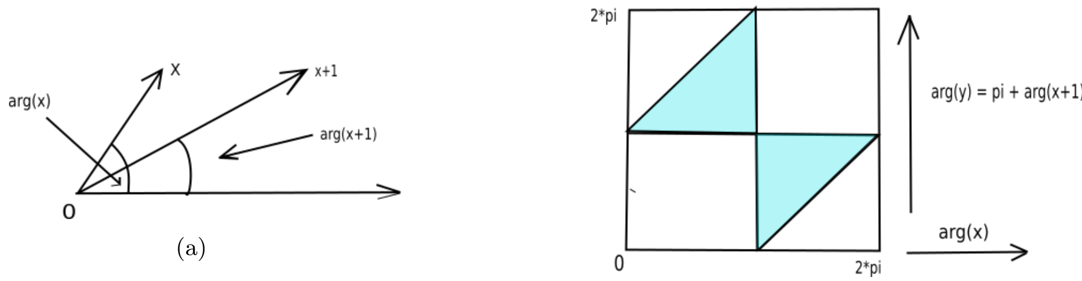

(a) (b)

Figure 4.2: Coemoeba of $x + y + 1 = 0$

4.5 Skeleton and the main theorem

Consider the fibration $\lambda : V_M \to V_{\text{trop}}$ with coamoeba fibers. The fibers of the interior poinst of 'E' are the closures of coamoeba of $z^a + z^b = 0$ where the the interval $(a, b) \subset \Delta$ is dual to 'E'. The fiber over 'v' is the closure of the coamoeba of $z^a + z^b + z^c = 0$, where 'v' is dual to a triangle (a, b, c) in Δ.

Over the barycentric neighborhood of a vertex 'v' $\in V_{\text{trop}}$, there are three canonical sections which are given by the points of mutual intersections of three fibers over the edges incident at 'v', see Figure 4.3. Denote by α_v, β_v and γ_v these 3 sections (colored Blue, Purple and Black in Figure 4.3).

We introduce two small opposite arcs A_e, B_e for the fiber at 'e', to glue two sections coming from neighboring vertices. In Figure 4.4 red arcs are used to glue two sections coming from two neighboring vertices. There are two ways to choose A_e, B_e. Denote by S^1_e the coamoeba circle over each 'marked e'.

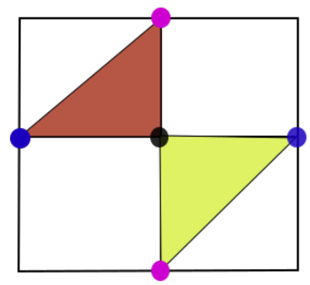

Figure 4.3: coamoeba of P_1 and 3 sections

.

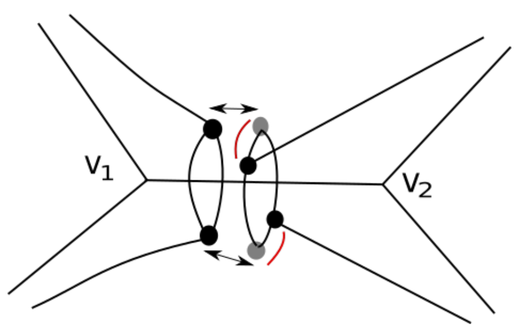

Figure 4.4: Two arcs, A_e and B_e

Definition 4.1. With all the notations described above, let

$$S := \left\{ \bigcup_{\text{vertices}} \alpha_v \cup \beta_v \cup \gamma_v \bigcup_{\text{`marked e'}} S^1_e \bigcup_{\text{`non-marked e'}} A_e \cup B_e \right\} \subset V_M.$$

S can also be interpreted as a fibration over V_{trop}.

We state and prove our main theorem.

Theorem 4.3. *With all notations as above, the set S is a deformation retract of V_M. In other words, S is a skeleton.*

Proof. We have two maps $\text{Arg} : V_M \to T^2$ and $\text{Log} : V_M \to V_{\text{trop}}$. The fiber of Log over 'v' is the coamoeba of $z^a + z^b + z^c = 0$. The closure of the coamoeba of $z^a + z^b + z^c = 0$ consists of two triangles, Yellow (Y) and Orange (O), see Figure 4.5. The inverse images $\text{Arg}^{-1}(Y) =$ 'Yellow Ball' and $\text{Arg}^{-1}(O) =$ 'Orange Ball', form 2-balls in the CW decomposition of $\text{Log}^{-1}(U), U \subset V_{\text{trop}}$ is a barycentric neighborhood of 'v'.

We contract these 2-balls as follows. At each 'v', suppose the edges 'ev' are oriented as shown in Figure 4.5 (right one). The incoming 'ev' corresponds to the boundaries 'ab' of both triangles. The boundary 'ab', colored blue, of the Yellow triangle corresponds to blue arc of the 'Yellow Ball'. Similarly for outgoing edges. We contract the 'Yellow Ball' starting from the part of 'blue' boundary. After contraction, we get a union of the red arc, the green arc and the sections a,b and c. This union forms a part of the set S. We

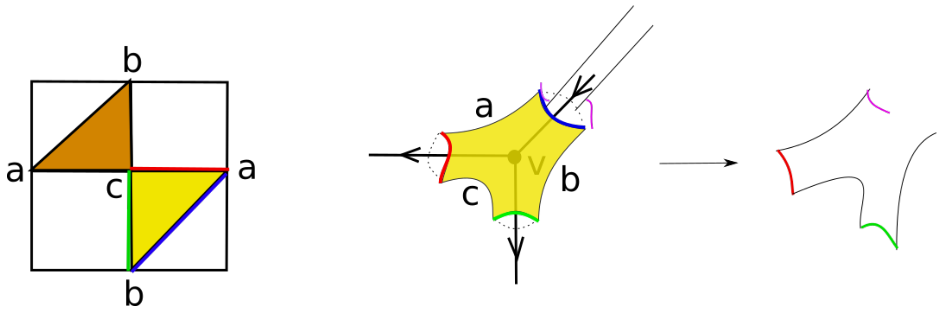

Figure 4.5: Contraction of 2-ball, 'Yellow Ball'

contract the 'Orange Ball' in similar fashion.

The orientation provides a partial ordering of the vertices of V_{trop}. Following this ordering make contraction steps described above. This gives the skeleton. $\square$

Chapter 5

Construction of skeleta: Surface case

Let $V_f \subset (\mathbb{C}^*)^3$ be the affine surface defined by a Laurent polynomial $f(z) = \sum_{j\in\Delta\cap\mathbb{Z}^3} a_j z^j$, where Δ is the Newton polytope. We consider a coherent triangulation of Δ, given by the map $\gamma : \Delta \cap \mathbb{Z}^3 \to \mathbb{R}$. The family of polynomials, $f_t(z) = \sum_{j\in\Delta} a_j t^{-\gamma(j)} z^j$ give a family of smooth affine surfaces V_t. As $t \to \infty$, their amoebas $A_t \subset \mathbb{R}^3$ converges in Hausdorff metric to a tropical surface V_{trop}. V_{trop} is a polyhedral complex. We assume that the triangulation of Δ is unimodular, see Definition 3.2. This is equivalent to smoothness of the tropical surface. We also get V_t converging in Hausdorff metric to the phase tropical surface V_∞. From now onwards, we call V_∞ as V_M for simplicity.

The family of polynomials, f_t can be considered as a single polynomial in $\mathbb{K}^*$. Let $V_{\mathbb{K}}$ be the affine surface defined by f_t in $(\mathbb{K}^*)^3$. Recall the map, $w := (\text{val}, \arg) : \mathbb{K}^* \to \mathbb{C}^*$ and the multiplicative group homomorphism

$W := \mathrm{Val} \times \mathrm{Arg} : (\mathbb{K}^*)^{n+1} \to (\mathbb{C}^*)^{n+1}$. V_M is the image of $V_{\mathbb{K}}$ under the map W, that is $V_M = W(V_{\mathbb{K}})$.

Consider V'_M described as a fibration, $V_M \to V_{\text{trop}}$ where the fiber over $x \in V_{\text{trop}}$ is a closure of the coamoeba of the polynomial whose Newton polytope is Δ', where Δ' is the polytope in the subdivision of Δ dual to the smallest strata in V_{trop}, which contains x.

Lemma 5.1. $V'_M = V_M$.

Proof. We have a projection $\mathrm{Val} : V_M \to V_{\text{trop}}$. Let $x \in V_{\text{trop}}$ and $\tau_{\Delta'} \subset V_{\text{trop}}$ containing x, where Δ' is the cell in the subdivision of Δ, dual to $\tau_{\Delta'}$. Suppose $\Delta' \cap \mathbb{Z}^3 = \{\alpha, \beta, \gamma\}$, then equation of V_f reduces to $a_\alpha + a^\beta + a^\gamma$ over $(\mathbb{C}^*)^3$ because the lower powers of a in $a_\alpha, a^\beta, a^\gamma$ are the same. $\square$

5.1 Barycentric subdivision and orientation

Consider the first barycentric subdivision of V_{trop}. We make the following notations.

For V_{trop}:

- $\mathbf{v}$ = vertex, $\mathbf{E}$ = edge and $\mathbf{F}$ = face.

For barycentric subdivision of V_{trop}:

- For vertices: $\mathbf{v}$ = vertex, $\mathbf{e}$ = barycenter of $\mathbf{E}$, $\mathbf{f}$ = barycenter of $\mathbf{F}$.

- For edges : **ev** = edge from **e** to **v**, **ef** = edge from **e** to **f**. Ordering of letters is not important, for example **ev** is the same as the **ve**.

To define a skeleton, we need an orientation on the edges of the barycentric subdivision. The orientation should satisfy the following properties:

1. At each **v**, edges **ev**'s should be oriented such that one of the four **ev**'s is incoming and the other three are outgoing from **v**.

2. At each **e**, if both **ev** incident at **e** are incoming to **e**, we call this **'marked e'**. There are 3 **ef**'s incident at **e**. We call **ef** incident at **'marked e'** a **'marked ef'**. We orient **'marked ef'** edges such that,

    - one is incoming and other two outgoing from **'marked e'**.
    - no more than one **ev** incident at **e** is oriented as outgoing from **e**.

3. We call **f** as **'marked f'** if all **'marked ef'** are oriented incoming at **f**. No more than one **'marked ef'** should be oriented as outgoing from **f**.

4. Infinite *ev* edges are oriented from ∞ to **e**.

Lemma 5.2. *The orientation with the properties 1, 2 and 3 mentioned above exists and the graphs of* ***evs*** *and the graph of* ***'marked ef'****s are acyclic.*

Proof. First we construct an orientation with the desired properties 5.1. We take a generic piecewise linear concave function $\Phi : \mathbb{R}^3 \to \mathbb{R}$. The gradi-

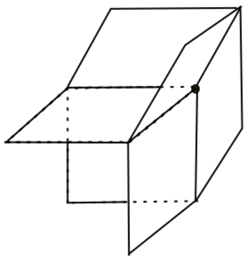

(a) Tropical surface of $z_1 + z_2 + z_3 + 1 = 0$

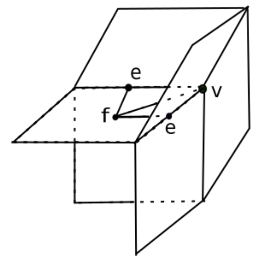

(b) First barycentric subdivision

Figure 5.1: Σ_2 in Figure 5.3a and subdivision in Figure 5.3b

ent flow of Φ induces an orientation on the edges **ev**'s of the barycentric subdivision. When we restrict Φ to any **F**, we have the following cases.

- Case I: When Φ assumes maximum value at an interion point of **F**. We take this point as baricenter of **F** and call it **f**.

- Case II: When Φ assumes maximum value at an interior point of **E**. We take this point the barycenter of **E** and call it **'marked e'**.

- Case III: When Φ assumes maximum value at a vertex **v**. There are two ways it could happen:

  – Subcase i : When Φ assumes maximum value at a vertex for a face **F**. Let **v** be the vertex. Two **E**s, say $\mathbf{E}_1$ and $\mathbf{E}_2$ incident at **v** are incoming at a vertex and other two, say $\mathbf{E}_3$ and $\mathbf{E}_4$ are outgoing from **v**. Let $\mathbf{F}_{12}$ be the face for which Φ assumes maximum value at **v**. Let $\mathbf{e}_1, \mathbf{e}_2$ and $\mathbf{f}_{12}$ be the baricenters of $\mathbf{E}_1, \mathbf{E}_2$ and $\mathbf{F}_{12}$ respectively. We take any one of $\{\mathbf{E}_1, \mathbf{E}_2\}$, say $\mathbf{E}_1$ and switch the orientation of the edge $\mathbf{e}_1\mathbf{v}$ making it going from $\mathbf{v}$ to $\mathbf{e}_1$. After the switch, both $\mathbf{ev}$'s incident at $\mathbf{e}_1$ are oriented towards $\mathbf{e}_1$. Thus $\mathbf{e}_1$ becomes **'marked e'**.

– Subcase ii: When Φ has maximum value at $\mathbf{v}$ for three $\mathbf{F}$s. Let $\mathbf{v}$ be the vertex. Then, three edges, say $\mathbf{E}_1, \mathbf{E}_2$ and $\mathbf{E}_3$ are incoming and $\mathbf{E}_4$ is outgoing from $\mathbf{v}_2$. Let $\mathbf{e}_1$, $\mathbf{e}_2$, $\mathbf{e}_3$ be the barycenters of of $\mathbf{E}_1, \mathbf{E}_2, \mathbf{E}_3$ respectively. Let $\mathbf{F}_{12}, \mathbf{F}_{23}$ and $\mathbf{F}_{13}$ be the faces with edges $\{\mathbf{E}_1, \mathbf{E}_2\}, \{\mathbf{E}_2, \mathbf{E}_3\}$ and $\{\mathbf{E}_1, \mathbf{E}_3\}$ respectively and $\mathbf{f}_{12}, \mathbf{f}_{23}, \mathbf{f}_{13}$ be their baricenters. We choose any one combination out of

$$\{\mathbf{E}_1, \mathbf{E}_2\}, \{\mathbf{E}_2, \mathbf{E}_3\}, \{\mathbf{E}_1, \mathbf{E}_3\}.$$

For example, we take $\{\mathbf{E}_1, \mathbf{E}_2\}$. We make a switch in the orientation of $\mathbf{e}_1\mathbf{v}$ so that it is oriented from $\mathbf{v}$ to $\mathbf{e}_1$. Similarly for edge $\mathbf{E}_2$. These two switches of the orientation give rise to two new **'marked e'**s.

Note that other possibilities: all $\mathbf{E}$s are incoming or all are outgoing at $\mathbf{v}$ cannot happen due to balancing condition V_{trop} should satisfy at a vertex.

Orientation of **ef** edges:

1. When we make a switch as in Subcase i for $\mathbf{E}_1$. At $\mathbf{e}_1$, we orient $\mathbf{e}_1\mathbf{f}_1$ going from $\mathbf{f}_1$ to $\mathbf{e}_1$ and other two oriented out from $\mathbf{e}_1$.

2. When we make two switchs of two edges $\mathbf{E}_1$ and $\mathbf{E}_2$ as in Subcase ii.

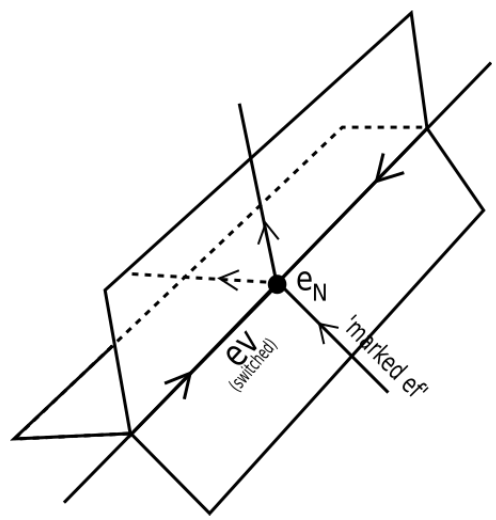

Figure 5.2: Orientation of **'marked ef'**.

At $\mathbf{e}_1$: We orient $\mathbf{e}_1\mathbf{f}_{13}$ as going from $\mathbf{f}_{13}$ to $\mathbf{e}_1$, and orient the other two as outgoing.

At $\mathbf{e}_2$: We orient $\mathbf{e}_2\mathbf{f}_{23}$ as going from $\mathbf{f}_{23}$ to $\mathbf{e}_2$ and orient the other two as outgoing.

3. When two **F**'s achieve maximum value at **e** so that two **ef**'s are incoming at **e**. In this case, we switch the orientation of one of these two incoming **ef**'s.

Next, we prove the claim that the graph with this orientation is acyclic. In particular, there are no cycles of **'marked ef'** edges.

Before the switch, we claim that there are no cycles of oriented **ev** edges. This is done by ordering such that **ef**'s are oriented according to values of Φ.

After the switch, there are no cycles of **E** edges since we make switch of

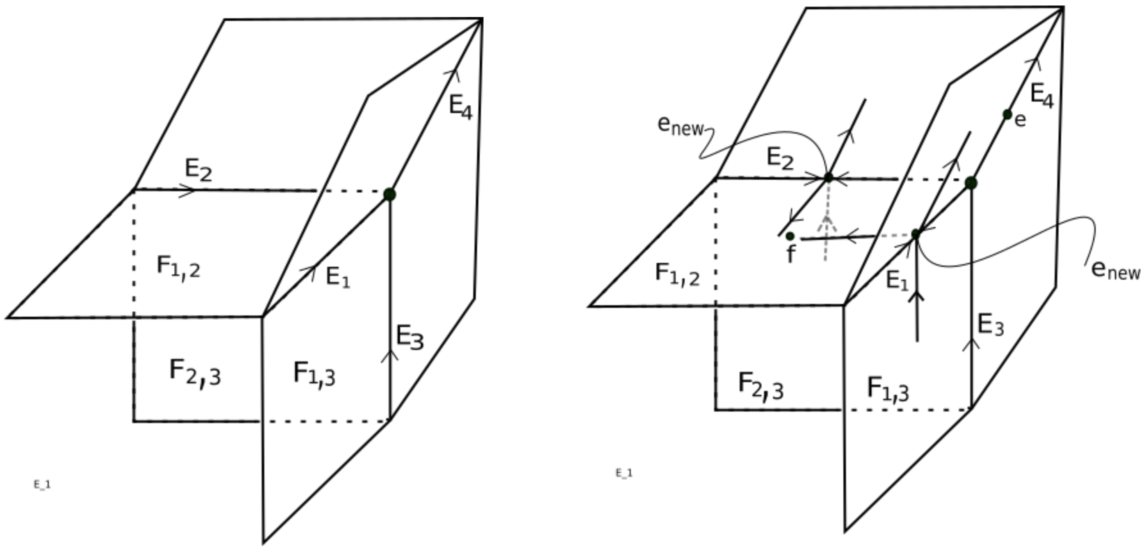

(a) One of the three possible orientations at $\mathbf{v}$.

(b) After the switch of orientation. Here $e_{\text{new}} = e_N$
.

Figure 5.3: Illustrating 3 incoming and 1 outgoing from a vertex

only half of $\mathbf{E}$.

We next claim that the graph of **'marked ef'** edges has no cycle. For Case II, we choose the barycenter $\mathbf{f}_{1,2}$ of $\mathbf{F}_{1,2}$ far from vertex $\mathbf{v}_2$ and the barycenter $\mathbf{e}_N$ of $\mathbf{E}_1$ close to $\mathbf{v}_2$ so that $\Phi(\mathbf{f}_{1,2}) < \Phi(\mathbf{e}_N)$. For Case III, we choose $\mathbf{f}_{1,2}$ very close to the vertex $\mathbf{v}_3$ and $\mathbf{e}_{N1}$ and $\mathbf{e}_{N2}$ such that $\Phi(\mathbf{f}_{1,2}) > \Phi(\mathbf{e}_{N1})$ and $\Phi(\mathbf{f}_{1,2}) > \Phi(\mathbf{e}_{N2})$. Similarly we choose $\mathbf{f}_{1,3}$ far away from $\mathbf{e}_{N1}$ such that $\Phi(\mathbf{f}_{1,3}) < \Phi(\mathbf{e}_{N1})$ and choose $\mathbf{f}_{2,3}$ and $\mathbf{e}_{N2}$ such that $\Phi(\mathbf{f}_{2,3}) < \Phi(\mathbf{e}_{N2})$. So, we have the inequalities, $\Phi(\mathbf{f}_{1,3} < \Phi(\mathbf{e}_{N1}) < \Phi(\mathbf{f}_{1,2})$ and $\Phi(\mathbf{f}_{2,3}) < \Phi(\mathbf{e}_{N2}) < \Phi(\mathbf{f}_{1,2})$. These choices make the graph of **'marked ef'**'s to be oriented according to the values of Φ. So it is acyclic.

It is possible that two **ef**'s are oriented towards $\mathbf{e}$ when two $\mathbf{F}$'s have maximum values at **e**. We make a switch in the orientation of one of them. This switch doesn't produce any new cycle of **'marked ef'** edges since the switched **'marked ef'** is oriented to a sink, **f**. □

5.2 Sections of Log : $V_M \to V_{\mathbf{trop}}$

The inverse image of a neighborhood of each $\mathbf{v} \in V_{\text{trop}}$ of Log : $V_M \to V_{\text{trop}}$ is the closure of the coamoeba of P_2. The coemoeba is the image under the map Arg : $(\mathbb{C}^*)^3 \to T^3$ defined by

$$\text{Arg}(z_1, z_2, z_3) = (\arg|z_1|, \arg|z_2|, \arg|z_3|).$$

The closure of the coamoeba of P_2 is cut out by six planes in the cube, see Figure 5.4. The inverse images of these planes under the map Arg are $2-$tori. Put $\arg(z_1) = x, \arg(z_2) = y$ and $\text{z}_3 = z$. These six planes are algebraically given by:

1. $x = \pi$ or plane SZJL,
2. $y = \pi$ or plane IHXQ,
3. $z = \pi$ or plane EGNU,
4. $y = x \pm \pi$ or planes SZXQ and IHJL,
5. $z = y \pm \pi$ or planes EIQU and GHXN,
6. $z = x \pm \pi$ or planes ESXL and JNZU.

Below, we have listed the points of intersecton among these planes (T^2). These points will be the seven sections $\alpha_v^i, i = 1, \ldots, 7$ we are going to use later for $\mathbf{v}$.

1. The intersection point of the planes: 1, 2 and 3 is O.

2. The intersection point of the planes: 2, 4 and 5 is I = H = X = Q.

3. The intersection point of the planes: 3, 5 and 6 is E=G = N = U.

4. The intersection point of the planes: 1, 4 and 6 is J =L = S = Z.

5. The intersection point of the planes: 1, 2, 5 and 6 is A = Y.

6. The intersection point of the planes: 2, 3, 4 and 6 is F = V.

7. The intersection point of the planes: 1, 3, 4 and 5 is K = T.

Each plane has 4 points out of those 7 points listed above. The following 4 points are associated with the plane $z = \pi$.

1. Point of intersection of planes 3, 2 and 1 is O;

2. Point of intersection of planes 3, 1, 4 and 5 is K = T

3. Point of intersection of planes 3, 2, 4 and 6 is F = V.

4. Point of intersection of planes 3, 5 and 6 is E = G = N = U.

Similarly, we can get 6 points over an interior point of $\mathbf{E}$. These are the points on the coamoeba over the edge $\mathbf{E}$. In Figure 5.7, we pair same colored dots to get those points.

5.3 Skeleta and main theorem

Definition 5.1. We have the fibration Log : $V_M \to V_{\text{trop}}$. Recall the notations, $\mathbf{v}$ = vertex, $\mathbf{E}$ = edge and $\mathbf{F}$ = face of V_{trop}.

1. Over every baricentric neighborhood of a vertex $\mathbf{v}$, we have 7 local sections, $\alpha_v^i, i = 1, \ldots, 7$, 6 local sections $\alpha_E^i, i = 1, \ldots, 6$ (out of those 7 sections) over an $\mathbf{E}$ and 4 local sections $\alpha_F^i, i = 1, \ldots, 4$ (out of those 7 sections) over a face, $\mathbf{F}$.
2. The fiber over **'marked f'** is a torus, T_f^2.
3. The fiber over non-marked $\mathbf{e}$ is 6 arcs, $A_e^i, i = 1, \ldots, 6$ to connect 6 sections on either side of $\mathbf{e}$ along $\mathbf{E}$, see Figure 5.7.
4. The fibers over interior points of non-marked **ef** are 4 arcs $A_{ef}^i, i = 1, \ldots, 4$ from the above 6 arcs to connect sections on either side of **ef**. For example, consider two neighboring vertices $\mathbf{v}_1$ and $\mathbf{v}_2$ as shown in Figure 5.10. Three affine planes 1, 2 and 3 are common to both vertices. On the left side of **ef** i. e. towards $\mathbf{v}_1$, the four sections are given by: $\{1, 3, B\}, \{1, 2, C\}, \{1, 3, A, C\}, \{1, 2, A, B\}$. On right side, these are given by $\{1, 3, B'\}, \{1, 2, C'\}, \{1, 3, A', C'\}, \{1, 2, A', B'\}$. We connect them in the order they are written down and introduce 4 little

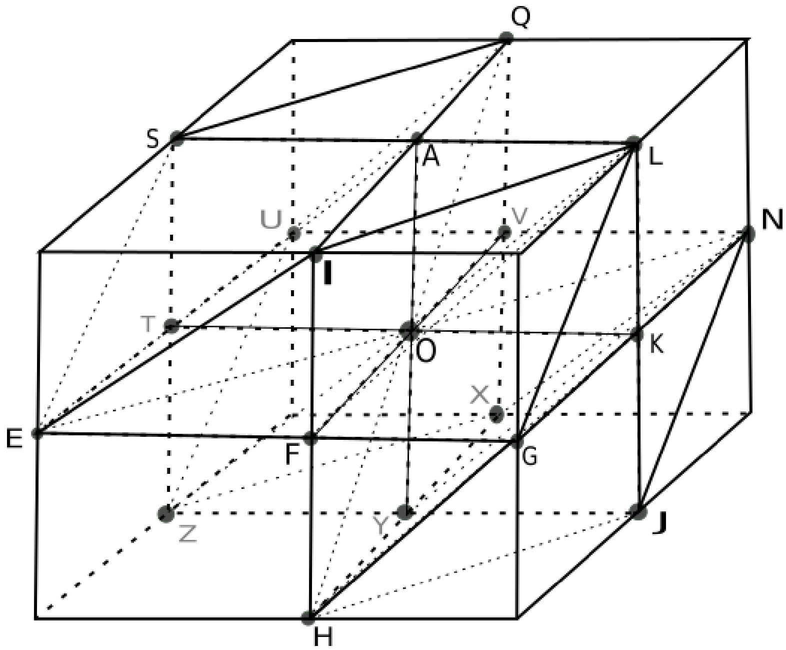

Figure 5.4: 7 sections over a vertex.

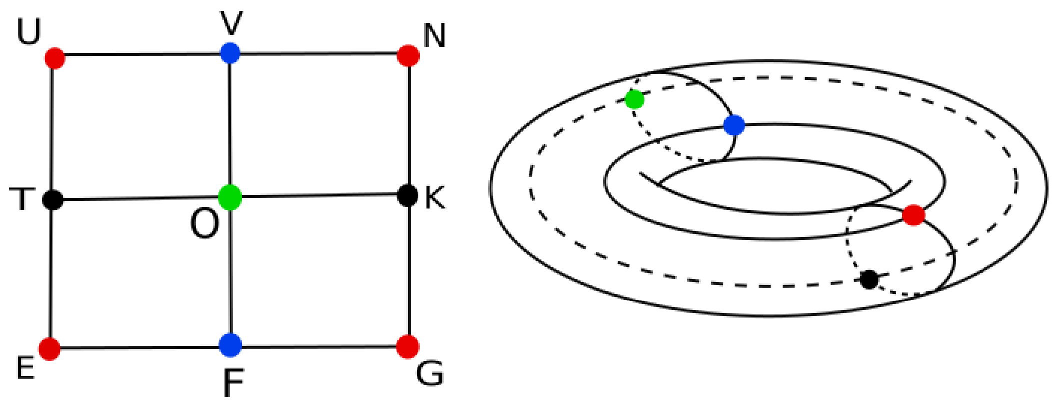

Figure 5.5: 4 local sections indicated as colored dots for the torus $z = \pi$.

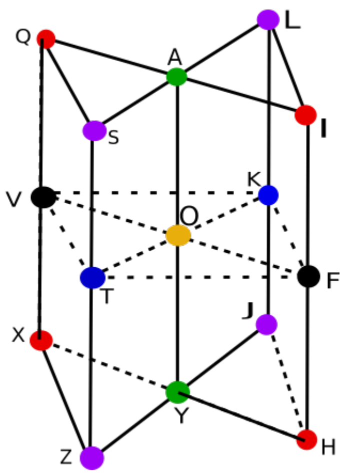

Figure 5.6: Two prisms: ALIHYJ and AQSXYZ and 6 sections: Red, Blue, Purple, Black, Orange and Green

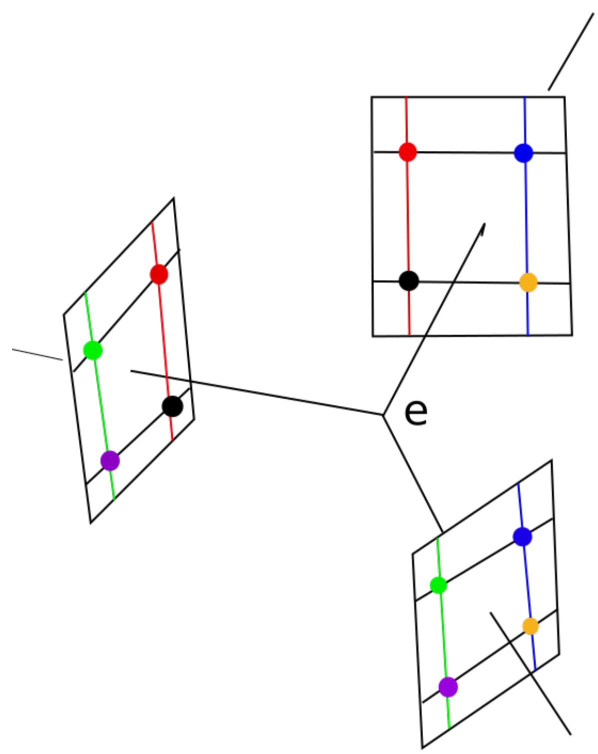

Figure 5.7: 6 Sections over vertex **e**

.

arcs $A^i_{ef}, i = 1, \ldots, 4$, parallel to **ef** to connect if they don't agree, see Figure 5.11. There are two ways to connect these sections.

5. At **'marked e'** we choose a fiber T^2 transversal to the edge **ev**. The fiber over **'marked e'** is three circles $S^i_{pe}, i = 1, \ldots, 3$ parallel to the edge **ev** and a transversal 2-dimensional coamoeba (intersection of transversal T^2 with original fiber at **e**), C_2 over **'marked e'**.

6. Over interior point of **'marked ef'**, the fiber is two circles S^1_{pef} parallel to **ef** and a transversal circle S^1_{tef}. By parallel and transversal circles, we mean, for example see Figure 5.11 those circles in the 2-torus, which don't intersect and the ones which intersect to each other.

7. Over non-marked **f**, two circles parallel to outgoing edge **'marked e'** from **f** and a transversal circle divide the fiber over **f** into 2 components, call them A and B. There are many other circles on the fiber, coming from **ef** edges and these circles further subdivide the fiber into many components. We pick two components A' and B', one lying in A and the other lying in B, see Figure 5.9. The fiber T^2_R over non-marked **f** is the complement of A' and B' in T^2 over **f**.

Definition 5.2. With all notations as described in Defintion 5.1, we denote

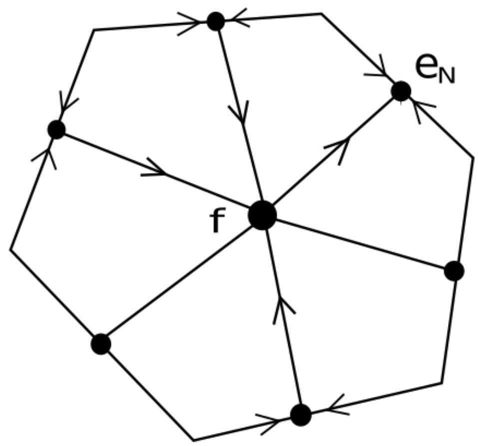

Figure 5.8: a possibile orientation at **f**

.

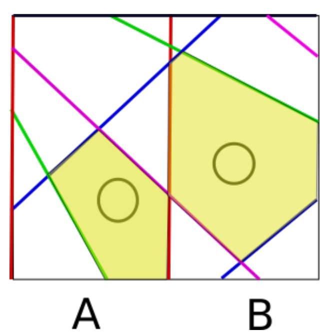

Figure 5.9: fiber over **f**, two vertical red circles and horizontal black circle divide T^2 into 2 components

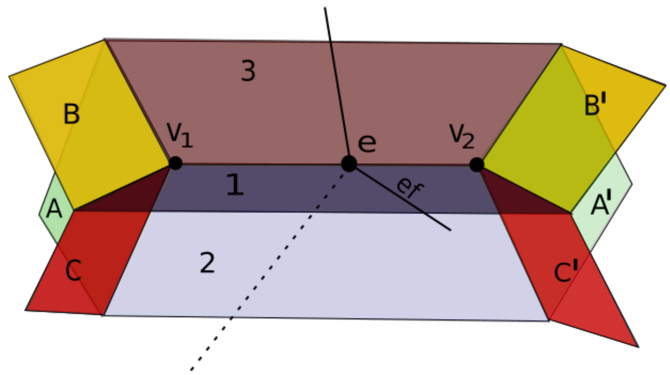

Figure 5.10: Two neighboring vertices

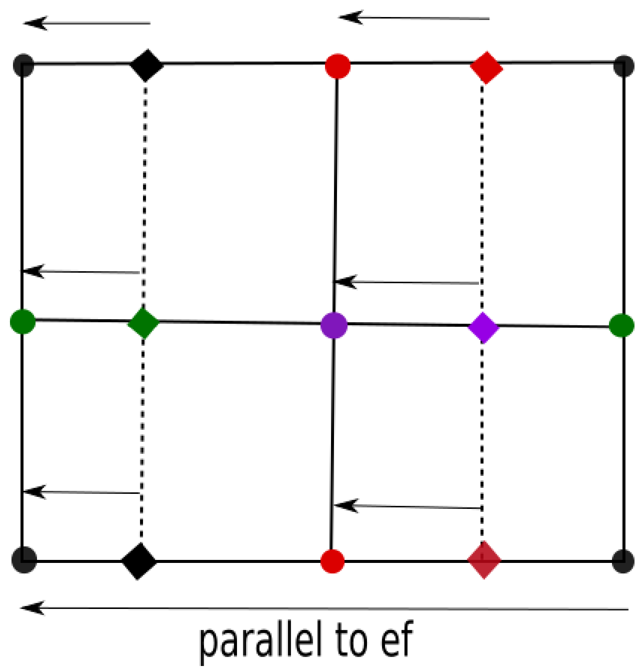

.

Figure 5.11: 4 arcs over non marked **ef** to connect 4 sections (a red, a black, a purple and a green) from either side of the **ef**. The black should connect to black by an arc parallel to **ef** and similar arcs to connect red to red, purple to purple and green to green.

by

$$S := \left\{ \bigcup_{\mathbf{v}} \alpha_v^i \bigcup_{\mathbf{f}} T_R^2 \bigcup_{\mathbf{e}} A_e^i \bigcup_{\text{'marked f'}} T_f^2 \bigcup_{\text{'marked e'}} S_{pe}^i \cup C_2 \bigcup_{\text{'marked ef'}} S_{pef}^i \cup S_{tef}^1 \right\}.$$

$S \subset V_M$. The index i for each component is defined above.

We now are going to state the main theorem.

Theorem 5.3 (main theorem)**.** *The set $S \subset V_M$ is a deformation retract of V_M.*

Before proving the theorem, we need to explain the decomposition of the coamoeba of 2-dimensional pair-of-pants P_2. The decomposition induces a CW structure on the 'tropical' pair-of-pants.

5.4 Decomposition of coamoeba of pair-of-pants

Let $T^3 = (\mathbb{R}/2\pi\mathbb{Z})^3$ be the 3-dimensional 'phase' torus. Let P_2 be the pair-of-pants, $z_3 + z_2 + z_1 + 1 = 0$. Take the coamoeba of P_2, $\mathrm{Arg}(P_2)$. Now we decompose this coamoeba into polytopes (octahedra).

We arrange the variables z_1, z_2, z_3 such that their arguments are non-decreasing:

$$0 \leq \arg(z_1) \leq \cdots \leq \arg(z_3) \leq 2\pi. \tag{5.1}$$

For any ordering 5.1, we denote the closure in T^3 of the set defined by these inequalities by $O_\sigma \subset C_2$, where σ is a permuation of the set $\{1, 2, 3\}$. For example, in Figure 5.12, the octahedra $EFIAOL$ is O_{0123}, $HFOKGL$ is O_{0321}. There are 4 more octahedra, $HOYJKN, ESTOAQ, QTUVOZ$ and $NOVXYZ$. Since there are 6 permutations of the set $\{1,2,3\}$, so are six octahedra.

The lower dimensional faces of these octahedra correspond to some equalities of the arguments in Equation 5.1. For example, $O_\sigma, \sigma = (01)23, 0(12)3, 01(23)$ where (12) means $\arg(z_1) = \arg(z_2)$ give the three faces of O_{0123}, namely EIF, AOE and LOF respectively. There are 12 such faces, which are listed below.

1. ΔLOF
2. ΔHOK
3. ΔEOA
4. ΔNOY
5. ΔOQT
6. ΔVOZ
7. $\Delta AIL = \Delta HJY$,
8. $\Delta EFI = \Delta UVQ$,
9. $\Delta ASQ = \Delta XYZ$,
10. $\Delta FHG = \Delta NVX$,
11. $\Delta GLK = \Delta EST$,
12. $\Delta JKN = \Delta TUZ$.

The vertices correspond to all variables $\arg(z_i)$ being real.

Lemma 5.4 (ref. Ilia Zharkov)**.** • *Let u_v be a baricentric neighborhood of $\boldsymbol{v}$. The preimage of octahedra O_σ, σ a permutation of* $\{1,2,3\}$, *in* $\operatorname{Log}^{-1}(u_v)$ *in V_M is a shellable PL 4-ball.*

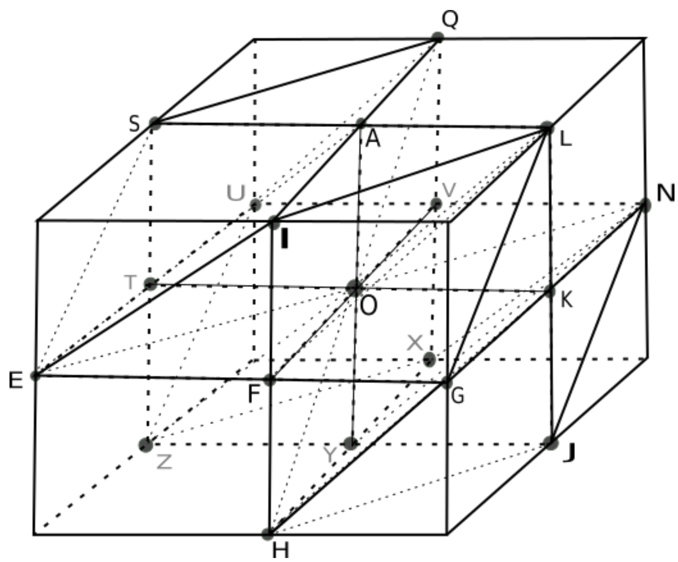

Figure 5.12: Decomposition of the Coamoeba of $1 + z_1 + z_2 + z_3 = 0$

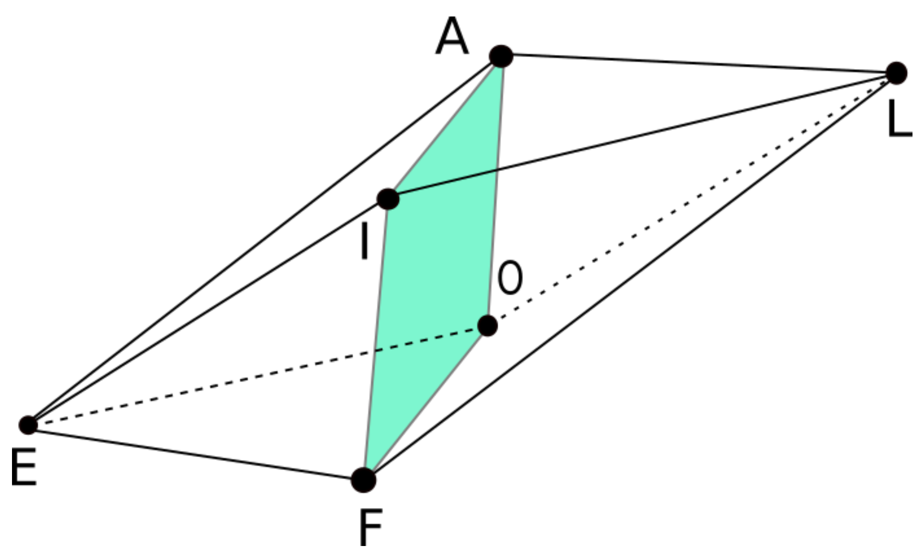

Figure 5.13: An octahedron EFIAOL

- *The preimage of the triangles listed in Section 5.4 in* $\mathrm{Log}^{-1}(u_v)$ *in* V_M *is a shellable 3-ball.*

Now we give the proof of the Theorem 5.3

Proof. **<u>Contraction at v:</u>** Let $\mathbf{v}$ be a vertex of V_{trop}. Let the orientation of **ev** edges at $\mathbf{v}$ be as shown in Figure 5.14b. The affine planes, $01, 02, 12$ in Figure 5.14b are dual to lines $01, 02, 12$ in Figure 5.14a respectively. They further correspond to planes (or T^2) $SLJZ : x = \pi$, $HIQX : y = \pi$, $IHJL$ and $SQXZ : y = x \pm \pi$ respectively from Figure 5.12.

Consider the octahedra $\sigma_{0123} = EFIAOL$. The inverse image $\mathrm{Log}^{-1}(\sigma_{0123}) = B_4$ of this octahedra is a 4-balll, Lemma 5.4). The part of the boundary of this ball is shown in Figure 5.15. This boundary lies in the closure of coamoeba of the edge 012 , see Figure 5.14b and is open to contract along with the 4-ball. Following the orientation at $\mathbf{v}$, we contract B_4 starting from the boundary given by intersection of inverse image of nbd of $\mathbf{e}$ with B_4, see Figure 5.15. The other balls given by the inverse images of the octahedra are contracted in the similar fashion. We perform this contraction at all vertices ordered by the value of Φ.

The 3-balls given by Arg^{-1}(triangle), where 'triangle' means one of the twelve triangles listed above are contracted thereafter.

<u>Contraction over 'marked ef'</u>: Recall that **'marked e'** is the vertex in

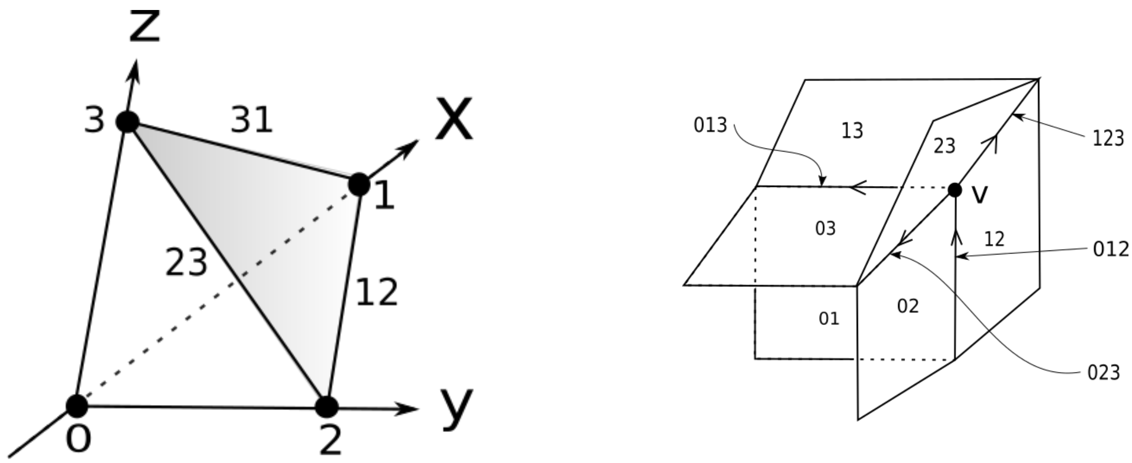

(a) Newton polytope (A standard simplex) of P_2

(b) Σ_2 of P_2

Figure 5.14

the barycentric subdivision where two **ev**s are incoming. Moreover, **'marked e'** is the vertex where one **'marked ef'** is oriented in and the other two oriented out from **'marked e'**, see Figure 5.16a. The fiber of Log over $\mathbf{e}_N$ is the closure of the coamoeba of $z^a + z^b + z^c = 0$. The coamoeba consists of two solid prisms as shown in Figure 5.16b, bounded by the planes $SLJZ, QIHX$ and $SQXZ, IHJL$ or planes C, B and D respectively. So the inverse image of Log of the neighborhood of **'marked e'** consists of two 3-balls. Each is given by attaching 3 leg cylinders to the faces of prism, see Figure 5.17.

We perform contractions for **'marked ef'** partially ordered by orientation of the graph of **'marked ef'**. The cell complex left after the contractions is precisely S. $\square$

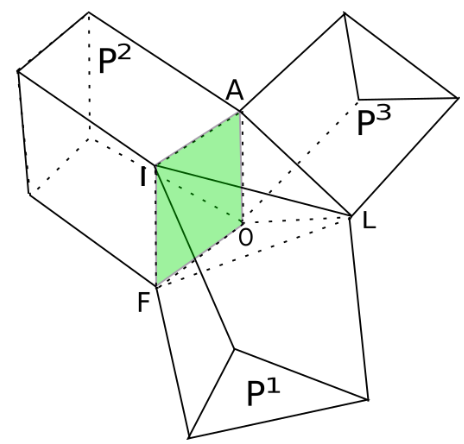

Figure 5.15: A part of the boundary of a 4-ball $EFIAOL$

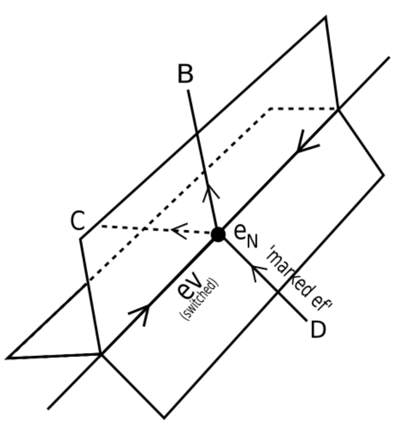

(a) Oriented **'marked ef'**

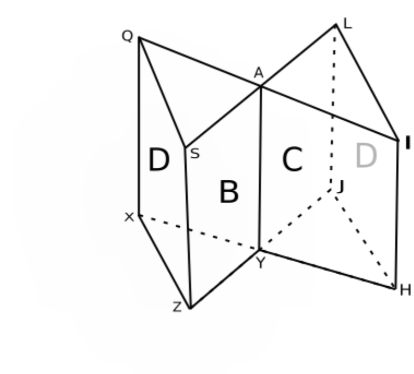

(b) Decomposition of fiber over e_N

Figure 5.16

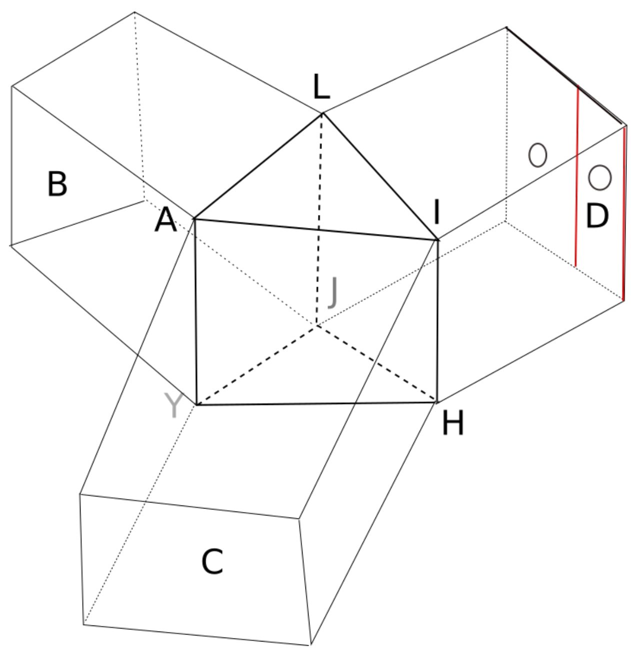

Figure 5.17: A 3-ball

Bibliography

[AF59] Aldo Andreotti and Theodore Frankel, *The lefschetz theorem on hyperplane sections*, Annals of Mathematics (1959), 713–717.

[Bat94] Victor V Batyrev, *Dual polyhedra and mirror symmetry for calabi–yau hypersurfaces in toric varieties*, J. Alg. Geom, Citeseer, 1994.

[Bor93] Lev Borisov, *Towards the mirror symmetry for calabi-yau complete intersections in gorenstein toric fano varieties*, arXiv preprint alg-geom/9310001 (1993).

[FLTZ11] Bohan Fang, Chiu-Chu Melissa Liu, David Treumann, and Eric Zaslow, *The coherent-constructible correspondence and homological mirror symmetry for toric varieties*, Geometry and analysis. No. 2, Adv. Lect. Math. (ALM), vol. 18, Int. Press, Somerville, MA, 2011, pp. 3–37.

[GKZ94] I.M. Gelfand, Mikhail Kapranov, and Andrei Zelevinsky, *Discriminants, resultants, and multidimensional determinants, mathematics: Theory & applications*, 1994.

[KKOY09] Anton Kapustin, Ludmil Katzarkov, Dmitri Orlov, and Mirroslav Yotov, *Homological mirror symmetry for manifolds of general type*, Central European Journal of Mathematics **7** (2009), no. 4, 571–605.

[Kon94] Maxim Kontsevich, *Homological algebra of mirror symmetry*, Proceedings of the International Congress of Mathematicians, Zürich (1994), 120–139.

[Kon09] ———, *Symplectic geometry of homological algebra*, Lecture at Mathematische Arbeitsgrunden (2009).

[Mik04a] Grigory Mikhalkin, *Amoebas of algebraic varieties and tropical geometry*, Different faces of geometry, Springer, 2004, pp. 257–300.

[Mik04b] ———, *Decomposition into pairs-of-pants for complex algebraic hypersurfaces*, Topology **43** (2004), no. 5, 1035–1065.

[Mik05] ———, *Enumerative tropical algebraic geometry in* ^{2}, Journal of the American Mathematical Society **18** (2005), no. 2, 313–377.

[Mik06] ———, *Tropical geometry and its applications*, International Congress of Mathematicians. Vol. II, Eur. Math. Soc., Zürich, 2006, pp. 827–852.

[MS15] Diane Maclagan and Bernd Sturmfels, *Introduction to tropical geometry*, vol. 161, American Mathematical Soc., 2015.

[Nis11] Mounir Nisse, *Complex tropical localization, and coamoebas of complex algebraic hypersurfaces*, Randomization, relaxation, and complexity in polynomial equation solving, Contemp. Math., vol. 556, Amer. Math. Soc., Providence, RI, 2011, pp. 127–144.

[NS11] Mounir Nisse and Frank Sottile, *Non-archimedean coamoebae*, Tropical and Non-Archimedean Geometry (Holetown, 2013) (2011), 73–91.

[PR04] Mikael Passare and Hans Rullgård, *Amoebas, Monge-Ampère measures, and triangulations of the Newton polytope*, Duke Math. J. **121** (2004), no. 3, 481–507.

[PT05] Mikael Passare and August Tsikh, *Amoebas: their spines and their contours*, Contemporary Mathematics **377** (2005), 275–288.

[RSTZ14] Helge Ruddat, Nicolò Sibilla, David Treumann, and Eric Zaslow, *Skeleta of affine hypersurfaces*, Geom. Topol. **18** (2014), no. 3, 1343–1395.

[STZ11] Nicolò Sibilla, David Treumann, and Eric Zaslow, *Ribbon graphs and mirror symmetry*, Selecta Mathematica (2011), 1–24.

[TZ11] David Treumann and Eric Zaslow, *Polytopes and skeleta*, arXiv preprint arXiv:1109.4430 (2011).

[Zha10] Ilia Zharkov, *Tropical theta characteristics*, Mirror Symmetry and Tropical Geometry: NSF-CBMS Conference on Tropical Geometry and Mirror Symmetry, December 13-17, 2008, Kansas State University, Manhattan, Kansas, vol. 527, American Mathematical Soc., 2010, p. 165.